








## A novel approach to understanding the link between supermassive black holes and host galaxies

GABRIEL SASSEVILLE <sup>1,2,3</sup> JULIE HLAVACEK-LARRONDO <sup>1,2,3</sup> SAMANTHA C. BEREK <sup>4,5</sup>  
GWENDOLYN M. EADIE <sup>4,5,6</sup> CARTER LEE RHEA <sup>1,2,3</sup> AARON SPRINGFORD <sup>7</sup> MAR MEZCUA <sup>8,9</sup> AND  
DARYL HAGGARD <sup>2,3,10,11</sup>

<sup>1</sup>Department of Physics, University of Montreal, Montreal, QC H2V 0B3, Canada

<sup>2</sup>Ciela - Montreal Institute for Astrophysical Data Analysis and Machine Learning, Montreal, QC H2V 0B3, Canada

<sup>3</sup>Centre de recherche en astrophysique du Québec (CRAQ), Canada

<sup>4</sup>Dunlap Institute for Astronomy & Astrophysics, University of Toronto, 50 St George Street, Toronto, ON M5S 3H4, Canada

<sup>5</sup>Data Sciences Institute, University of Toronto, 17th Floor, Ontario Power Building, 700 University Ave, Toronto, ON M5G 1Z5, Canada

<sup>6</sup>Department of Statistical Sciences, University of Toronto, 9th Floor, Ontario Power Building, 700 University Avenue, Toronto, ON M5G 1Z5, Canada

<sup>7</sup>Toronto, Ontario, Canada

<sup>8</sup>Institute of Space Sciences (ICE, CSIC), Campus UAB, Carrer de Magrans, 08193 Barcelona, Spain

<sup>9</sup>Institut d'Estudis Espacials de Catalunya (IEEC), Edifici RDIT, Campus UPC, 08860 Castelldefels (Barcelona), Spain

<sup>10</sup>Department of Physics, McGill University, 3600 rue University, Montréal, QC H3A2T8, Canada

<sup>11</sup>Trottier Space Institute at McGill, 3550 rue University, Montréal, QC H3A2A7, Canada

### ABSTRACT

The strongest and most universal scaling relation between a supermassive black hole and its host galaxy is known as the  $M_{\bullet} - \sigma$  relation, where  $M_{\bullet}$  is the mass of the central black hole and  $\sigma$  is the stellar velocity dispersion of the host galaxy. This relation has been studied for decades and is crucial for estimating black hole masses of distant galaxies. However, recent studies suggest the potential absence of central black holes in some galaxies, and a significant portion of current data only provides upper limits for the mass. Here, we introduce a novel approach using a *Bayesian hurdle model* to analyze the  $M_{\bullet} - \sigma$  relation across 244 galaxies. This model integrates upper mass limits and the likelihood of hosting a central black hole, combining logistic regression for black hole hosting probability with a linear regression of mass on  $\sigma$ . From the logistic regression, we find that galaxies with a velocity dispersion of 11, 34 and 126 km/s have a 50%, 90% and 99% probability of hosting a central black hole, respectively. Furthermore, from the linear regression portion of the model, we find that  $M_{\bullet} \propto \sigma^{5.8}$ , which is significantly steeper than the slope reported in earlier studies. Our model also predicts a population of under-massive black holes ( $M_{\bullet} = 10 - 10^5 M_{\odot}$ ) in galaxies with  $\sigma \lesssim 127$  km/s and over-massive black holes ( $M_{\bullet} \geq 1.8 \times 10^7$ ) above this threshold. This reveals an unexpected abundance of galaxies with intermediate-mass and ultramassive black holes, accessible to next-generation telescopes like the Extremely Large Telescope.

*Keywords:* Interdisciplinary astronomy (804), Astrostatistics (1882), Bayesian statistics (1900), Hierarchical models (1925),  $M_{\bullet} - \sigma$  relation (2026), Black holes (162), Galaxies (573), Black hole physics (159)

### 1. INTRODUCTION

The stellar velocity dispersion ( $\sigma$ ) of the bulge of a galaxy correlates strongly with the mass ( $M_{\bullet}$ ) of the supermassive black hole (BH) at its center. This relation, known as the  $M_{\bullet} - \sigma$  relation, has been observed empirically for decades (e.g. Merritt 1999; Ferrarese & Merritt 2000; Gültekin et al. 2009; Thater et al. 2019; Dullo et al. 2021) and takes the form of  $M_{\bullet} \propto \sigma^{5.4}$  (e.g.

van den Bosch 2016) for galaxies in the local Universe. It is considered a dynamical scaling relation. The mere existence of this correlation suggests coevolution between supermassive BHs and their host galaxies (e.g. Kormendy & Ho 2013). Indeed, the region within which the gravitational potential of the BH dominates the gravitational potential of the host galaxy, known as the sphere of influence, is significantly smaller (e.g.  $\approx 0.8$  parsec for

a BH with mass  $10^6 M_\odot$ ) than the size of its host galaxy which extends to dozens of kpc (e.g. Merritt et al. 2009, Kormendy & Ho 2013). The use of this dynamical scaling relation has proven to be crucial in estimating BH masses in distant galaxies at  $z > 0.1$  (e.g. Salviander & Shields 2013), for which it is difficult or impossible to obtain high resolution data for direct BH mass measurements with current telescopes.

Although the scatter in the  $M_\bullet - \sigma$  relation is low (0.40 dex) for high-mass BHs with  $M_\bullet \geq 10^6 M_\odot$ , it does not succeed in fitting the data at the low-mass end, where it rather follows  $M_\bullet \propto \sigma^{3.32}$  (e.g. Xiao et al. 2011). Thus, little is known about the transition region that lies between high and low velocity dispersion galaxies. This region corresponds to the range of BH masses for which there is a change in the slope of the  $M_\bullet - \sigma$  relation (e.g. Martin-Navarro & Mezcua 2018). Furthermore, some observational data suggest the lack of a central BH in some galaxies (e.g. Merritt et al. 2001, Gebhardt et al. 2001, Valluri et al. 2005, Coccato et al. 2006, Lyubenova et al. 2013, Nguyen et al. 2014), a phenomenon which is not predicted by the  $M_\bullet - \sigma$  relation. The lack of BHs in these galaxies, however, could be due to observational limits. For example, some dwarf galaxies thought to lack a central BH were recently found to have active galactic nuclei (AGN) once observational and estimation techniques improved (e.g. Mezcua et al. 2018a, Baldassare et al. 2020, Mezcua & Sánchez 2020, Reines 2022). Thus, we cannot say with certainty that some galaxies lack a central BH, and instead have upper limits on BH mass.

A better understanding of the transition mass as well as a detailed comparison of the low-mass and high-mass regions of the  $M_\bullet - \sigma$  relation could shed light on the BH-galaxy coevolution and the possible lack of a central BH in some dwarf galaxies. More precisely, the extension of the  $M_\bullet - \sigma$  relation to the low-mass regime could imply that the growth regulation in dwarf galaxies is driven by BH feedback, rather than supernova feedback (e.g. Efstathiou 2000, Stinson et al. 2009, Dashyan & Dubois 2020, Barai & Pino 2018, Baldassare et al. 2020).

Various methods have been used to model the  $M_\bullet - \sigma$  relation in previous studies, such as the bivariate linear regression routine from Akritas & Bershady (1996) used in Ferrarese & Merritt (2000) or the linear regression routines from Kelly (2007) used in van den Bosch (2016). Whilst Ferrarese & Merritt (2000) included uncertainties on both predictor and response variables (independent and dependent variables, respectively), they performed the regression on a sample of only 12 supermassive BHs where upper limits were excluded. On the other hand, van den Bosch (2016) included upper limits

and uncertainties on BH mass measurements, but their model was strictly linear in the log space and did not account for the potential lack of BHs in dwarf galaxies. The potential lack of a central BH was considered in Gültekin et al. (2009). They treated the probability of having no central BH as a constant value  $P_0$  and included it directly in the likelihood of their maximum likelihood estimation (MLE) technique for fitting (see appendix A of Gültekin et al. 2009). The problem with this assumption is that it may not hold for higher velocity dispersion galaxies, as it may be easier for them to form BHs (e.g. Haidar et al. 2022).

More recently, a novel fitting technique was used in Eadie et al. (2022) and Berek et al. (2023) to model the relationship between a globular cluster (GC) system’s mass and its host galaxy’s stellar mass, that allowed for the inclusion of zero GC counts in some galaxies. This model, known as a *Bayesian hurdle model*, which we will refer to as the hurdle model (e.g. Bürkner 2017), combines both binary and continuous data for the best fit. The hurdle model simultaneously modelled both (1) the probability of a galaxy containing a GC system, and (2) the linear relation between the mass of that system and the host galaxy’s stellar mass. They found that this technique was able to accurately model the data and provide them with new insights on the transition mass region ( $10^5 - 10^8 M_\odot$ ) where galaxies go from having no GC system to having one. Their findings suggest that the mass of GCs within this region are subject to large scatter and that the least massive GCs are likely to disappear due to dynamical evolution.

Here, we apply a similar hurdle model to the  $M_\bullet - \sigma$  relation. Our reasons for doing this are twofold: (1) the data from a statistical perspective is strikingly similar to that in Eadie et al. (2022) and Berek et al. (2023), and (2) the hurdle model overcomes many of the aforementioned issues of fitting the  $M_\bullet - \sigma$  relation. The novelty of the method is that it allows us to take into account systems that may not have a BH, without assuming a constant probability for the BH occupation. We also modify the hurdle model to include measurement uncertainties on BH mass measurements as well as uncertainties on upper limits. This task is not trivial as the uncertainties on the upper limits are heteroskedastic, but could provide valuable insight regarding this scaling relation (e.g. Eadie et al. 2022).

Our results show that considering upper limits and uncertainties on BH mass measurements tends to drag the high-mass end of the curve upwards and the low-mass end of the curve downwards while maintaining a similar trend for the transition region. If correct, the new behavior of the  $M_\bullet - \sigma$  relation at the low-mass

and high-mass end would have significant implications for our understanding of the coevolution between BHs and galaxies.

This paper is structured as follows. In Section 2, we present the observational data. In Section 3, we describe the hurdle model and its application to our dataset. Afterwards, we consolidate both binary and continuous distributions by applying this model to our sample. In Section 4, possible physical interpretations of our results as well as a comparison with previous results are presented. We finish with Section 5, in which we summarize our findings.

Throughout this paper, a flat concordance cosmology with  $H_0 = 70$  km/s and  $\Omega_m = 0.3$  is adopted.

## 2. OBSERVATIONAL SAMPLE

Our sample is comprised of 244 galaxies for which the central BH masses have been dynamically measured or temporally resolved (see Baldassare et al. 2015, Baldassare et al. 2016, van den Bosch 2016, Krajnović et al. 2018, Thater et al. 2019 and Baldassare et al. 2020). All BH masses along with their uncertainties are listed in Tables B1 and B2. The details of how we compiled these data will be explained next.

The BH mass measurements are done using four different methods: gas dynamics, stellar dynamics, megamasers and reverberation mapping. The first method relies on measuring gas dynamics at the galactic center, more precisely the rotational velocity of ionized gas surrounding the BH. This measurement can then be separated into its two sources, the gravitational potential from the central BH and the extended matter distribution of the galaxy’s stellar component (see Kormendy & Ho 2013, Yoon 2017). The second method is based on resolving stellar kinematics near the galactic center, rather than gas dynamics (see Siopis et al. 2009, McConnell et al. 2012, Kormendy & Ho 2013). The third method uses the rotation curves of  $H_2O$  megamaser disks formed in some AGN. These rotation curves follow a Keplerian law, which makes it relatively simple to determine the central BH mass (see Gao et al. 2016, Greene et al. 2016, Kuo et al. 2018). The final method relies on estimating the radius of the broad-line region by measuring time lags between the AGN’s continuum fluctuations. With this radius, the central BH mass can be found via the Virial theorem, assuming that the motion of the gas in the broad-line region is dominated by the BH’s influence (see Bentz et al. 2010; Grier et al. 2013; Baldassare et al. 2020).

Our data sample includes a large number of upper limits in addition to robust measurements, but does not include lower limits on BH mass measurements. The

diversity of our sample highlights the importance of including measurement uncertainties in the model. The various methods have different systematic uncertainties; megamasers have the smallest uncertainty (e.g. Gao et al. 2016, Kuo et al. 2018) and reverberation mapping is the most uncertain, as it relies on assuming the broad-line region’s geometry (e.g. Grier et al. 2013).

Our compilation is comprised of a total of 244 BHs with 2MASS growth curves and reliable velocity dispersions at redshifts up to  $z \approx 0.1$ . An additional 64 BHs are compiled in Table B2, but are omitted from the fits due to various reasons such as the lack of 2MASS growth curves, the lack of a measured velocity dispersion or due to them being significant outliers in the Fundamental Plane (FP) of BH accretion (see Merloni et al. 2003, van den Bosch et al. 2016, Gültekin et al. 2019). The 2MASS growth curves are essential because they provide global photometric properties necessary for evaluating BH masses and galaxy properties in the context of the Virial Theorem and the FP (e.g. van den Bosch 2016). Furthermore, the removal of significant outliers (galaxies NGC2139 and NGC4636) to the FP helps eliminate potential biases that may stem from systematic measurement errors, ensuring a more reliable analysis (e.g. van den Bosch 2016). Details on the omissions are discussed further in van den Bosch (2016). Including the upper limits is important because it allows us to gain insight on the low-mass end of the  $M_\bullet - \sigma$  relation, considering that 14 of the 24 BHs with masses  $\leq 10^6 M_\odot$  included in our fit are upper limits (e.g. Beifiori et al. 2009).

### 2.1. BH masses

Among the 244 BHs included in this paper, the mass measurements of 230 of them are taken from the compilation presented in van den Bosch (2016), which, in turn, were obtained from Merritt & Ferrarese (2001), Gebhardt et al. (2001), Valluri et al. (2005), Beifiori et al. (2009), Barth et al. (2009), Gültekin et al. (2009), Seth et al. (2010), Kormendy et al. (2010), Beifiori et al. (2012), Neumayer & Walcher (2012), McConnell & Ma (2013), Kormendy & Ho (2013), Lyubenova et al. (2013), Scharwächter et al. (2013), De Lorenzi et al. (2013), Onken et al. (2014), Gültekin et al. (2014), Nguyen et al. (2014), Seth et al. (2014), Walsh et al. (2015), Yıldırım et al. (2015), Onishi et al. (2015), Bentz & Katz (2015), Walsh et al. (2016), Barth et al. (2016), Thomas et al. (2016), Greene et al. (2016), Saglia et al. (2016), Onishi et al. (2016). Added to this are three BH masses from Krajnović et al. (2018) and one from Thater et al. (2019), all of which were measured using stellar dynamics. An additional eight BH masses from Baldassare

et al. (2020), one from Baldassare et al. (2015) and one from Baldassare et al. (2016) that were temporally resolved using reverberation mapping are included in the sample. This results in 244 BHs included in the regression.

We also note that BH masses are scaled by a factor  $\langle f \rangle = 4.31 \pm 1.05$  if they have been measured using Virial methods (e.g. Grier et al. 2013). Indeed, this virial factor accounts for the unknown geometry of the broad-line region, thus giving rise to a higher uncertainty than dynamical methods. Nevertheless, these methods are essential as they allow us to populate the low-mass end of our dataset. Statistical uncertainties on BH mass measurements are used when available. Otherwise, systematic uncertainties on the estimation technique are employed (e.g.  $\sim 0.4$  dex for the 8 BH masses in Baldassare et al. 2020) which are usually greater than the measurement uncertainty, acting as an overestimated boundary.

We use a  $3\sigma_x$  confidence level on BH mass measurements in our model, meaning the data is within 3 standard deviations ( $\sigma_x$ ) from the mean, or rather 99.7% of the data lies within the uncertainties, and we assume that they are Gaussian. Therefore, the uncertainties from the literature, as listed in Tables B1 and B2, have been scaled to  $3\sigma_x$  confidence levels (i.e. 99.7%) for all regression purposes. This assumption relies on the central limit theorem (e.g. Feller 1968, Billingsley 1995).

## 2.2. Velocity dispersions

For all objects, we prioritize the effective stellar velocity dispersion ( $\sigma_e$ ) over the central velocity dispersion ( $\sigma_c$ ). This is done because  $\sigma_e$  is the closest to the second moment of the 3D velocity tensor inside the half-light radius, which is the optimal measurement (e.g. van den Bosch 2016). We use the definition for  $\sigma_e$  from Gültekin et al. (2009):

$$\sigma_e = \frac{\int_0^{R_e} (\sigma^2 + V^2) I(r) dr}{\int_0^{R_e} I(r) dr} \quad (1)$$

where  $I(r)$  is the surface brightness of the galaxy,  $R_e$  is the effective radius and  $V$  is the rotational component of the spheroid. This is done to avoid inconsistencies in the data, although Gültekin et al. (2009) argues that there is no systematic bias to high or low values when comparing  $\sigma_e$  to  $\sigma_c$ . Thus, when the effective velocity dispersion is unavailable, the central velocity dispersion from HyperLeda<sup>1</sup> is used. All velocity dispersions along with their uncertainties are listed in Tables B1 and B2.

<sup>1</sup> See <http://leda.univ-lyon1.fr/>

## 3. MODEL AND METHODS

Hurdle models are a class of generalized linear models (GLMs; see e.g. de Souza et al. 2015b, Elliott et al. 2015, de Souza et al. 2015a) that allow the accurate modeling of data when zeros are present, i.e. when the response variable takes on values of zero in the dataset. Thus, they operate under the GLM framework, first introduced in Nelder & Wedderburn (1972), in which a link function  $g$  connects the expected value of the response  $\mathbf{Y}$  to the linear predictor  $\mathbf{X}\boldsymbol{\beta}$ :

$$g(E(\mathbf{Y})) = \mathbf{X}\boldsymbol{\beta}. \quad (2)$$

Hurdle models also allow the modeling of binary and continuous data in a two-step approach, as they use two distinct parts to describe a random variable. The first portion models the probability that a random variable, central BH mass in our case, reaches the value of zero or not using logistic regression (Section 3.1). The second part models the value of the random variable, using linear regression (Section 3.2), if a nonzero value was reached in the first portion (e.g. Zuur et al. 2009). The binary portion is considered to be the 'hurdle' that must be overcome to attain a nonzero value (e.g. Hilbe et al. 2017, Eadie et al. 2022).

We implement the hurdle model with the Bayesian Regression Models using Stan (`brms`) package in the R Statistical Software Environment (e.g. Bürkner 2017, R Core Team 2021). The `brms` package automatically translates the model into the Stan language and compiles code into C++ for efficient sampling. Stan (e.g. Carpenter et al. 2017) uses a No-U-Turn sampler, a method introduced in Hoffman & Gelman (2011) that has been optimized to allow for efficient high-dimensional sampling (e.g. Betancourt 2018). The Bayesian inference process is performed on samples approximating the posterior distribution, specifically a Markov chain of model parameters.

The next subsections define the two part model as well as our method of including uncertainties and upper limits in the model.

### 3.1. Logistic Regression

Logistic regression, a type of GLM, operates under the framework described in Section 3. In logistic regression, the response for variable  $i$  is assumed to follow a Bernoulli distribution with probability of success  $p_i$ , and probability of failure  $1 - p_i$  (e.g. Evans & Peacock 2000). When assuming that our response variables  $\mathbf{Y}$  are Bernoulli distributed, we obtain  $E(\mathbf{Y}) = \mathbf{p}$ . Combining this result with Equation (2), we obtain:

$$\mathbf{p} = g^{-1}(\mathbf{X}\boldsymbol{\beta}) \quad (3)$$



We use a *logit* link function to map the linear predictor term  $\mathbf{X}\boldsymbol{\beta}$  from the unconstrained space  $]-\infty, \infty[$  to the constrained space  $[0, 1]$  (e.g. [de Souza et al. 2015b](#)). When doing so, Equation (3) becomes:

$$\mathbf{p} = \text{logit}^{-1}(\mathbf{X}\boldsymbol{\beta}) = \frac{1}{1 + e^{-\mathbf{X}\boldsymbol{\beta}}} \quad (4)$$

As we are only interested in the case with one predictor variable, Equation (4) is simplified to:

$$p_i = \frac{1}{1 + e^{-(\beta_0 + \beta_1 X_i)}} \quad (5)$$

The two parameters  $\beta_0$  and  $\beta_1$  are obtained by the means of Bayesian inference (e.g. [Albert 2009](#), [van de Schoot et al. 2021](#)) where the likelihood is defined as in [Eadie et al. \(2022\)](#):

$$\mathcal{L}(\boldsymbol{\beta}; \mathbf{x}, \mathbf{y}) = \prod_i^N p_i^{y_i} (1 - p_i)^{1 - y_i} \quad (6)$$

with each  $p_i$  defined by Equation (5).

### 3.2. Linear Regression

Linear regression is used to model the relationship between the predictor variable and the nonzero values of the response variable resulting from the binary portion of the model. It is performed through Bayesian inference, based on the same framework as described in [Eadie et al. \(2022\)](#) and [Berek et al. \(2023\)](#), and results in the following form:

$$E[\log M_{\bullet}] = (\gamma_0 + \gamma_1 \log \sigma) \quad (7)$$

where  $\gamma_0$  and  $\gamma_1$  are the parameters of the linear regression.

Sections 3.2.1 and 3.2.3 describe the linear regression models used for treating precise mass measurements and upper limits, respectively. The details of including uncertainties and upper limits in this portion of the model are discussed in Section 3.2.2.

#### 3.2.1. Lognormal Distribution

Our method uses the same framework as described in the previous subsection, where we use  $\boldsymbol{\gamma}$  instead of  $\boldsymbol{\beta}$  to avoid confusion:

$$E(\mathbf{Y}) = g^{-1}(\mathbf{X}\boldsymbol{\gamma}) \quad (8)$$

The canonical link function can be used to map the linear predictor term  $\mathbf{X}\boldsymbol{\gamma}$  from the unconstrained space  $]-\infty, \infty[$  to the zero-truncated space  $]0, \infty[$  (e.g. [Hardin et al. 2007](#)). Thus, Equation (8) becomes:

$$E(\mathbf{Y}) = \mathbf{X}\boldsymbol{\gamma} \quad (9)$$

The assumption for the normal model described in [Nelder & Wedderburn \(1972\)](#) still holds for the lognormal model as long as the natural log of the response variable is taken prior to modeling. This assumption is as follows:

$$E(\mathbf{Y}) = \boldsymbol{\mu} \quad (10)$$

Combining the two previous results, we obtain the following:

$$\boldsymbol{\mu} = \mathbf{X}\boldsymbol{\gamma} \quad (11)$$

Although the generalization to multiple predictors is quite simple, we are solely interested in the case with one predictor since we are only studying the relation between  $M_{\bullet}$  and  $\sigma$ , without taking into account other factors. Thus, Equation (11) is simplified:

$$\boldsymbol{\mu}_i = (\gamma_0 + \gamma_1 X_i) \quad (12)$$

Once again, the two parameters  $\gamma_0$  and  $\gamma_1$  are obtained via Bayesian inference (e.g. [Albert 2009](#), [van de Schoot et al. 2021](#)) where the likelihood is defined as in [Hardin et al. \(2007\)](#):

$$\mathcal{L}(\boldsymbol{\gamma}; \mathbf{x}, \mathbf{y}) = \prod_i^N \frac{1}{\sigma\sqrt{2\pi}} \frac{1}{y_i} \exp\left(-\frac{1}{2} \left(\frac{\ln(y_i) - \mu_i}{\sigma}\right)^2\right) \quad (13)$$

#### 3.2.2. Uncertainties and Upper Limits

The values that overcome the hurdle are typically addressed by assuming that they are lognormally distributed, as demonstrated in previous works (e.g. [Eadie et al. 2022](#), [Berek et al. 2023](#)). In our approach, we present a novel methodology by distinguishing between precise mass measurements and nonzero upper limits, using distinct distributions for each. Specifically, we model precise mass measurements using a lognormal distribution, consistent with the approaches described in [Eadie et al. \(2022\)](#) and [Berek et al. \(2023\)](#).

In our treatment of upper limits, we explored several options to accurately model the uncertainty and nature of these limits, including the use of exponential and Lévy distributions. However, we found that a mixture model provided a more representative description. This model treats the upper limits as either being close to the limit or close to the established relation, allowing for more flexibility. The model uses a truncated normal distribution to represent data points near the detection limit and a lognormal distribution for values closer to the established mass relation. The weight between these two distributions, represented by the parameter  $\lambda$ , is learned

from the data itself. This enables the model to adapt and more realistically represent cases where upper limits correspond to true masses near the relation.

### 3.2.3. Mixture Model for Upper Limits

For upper limits, we adopt a mixture model approach. The same framework and methodology from Section 3.2 applies, except the likelihood function now blends log-normal and truncated normal distributions:

$$\mathcal{L}(\boldsymbol{\gamma}, \boldsymbol{\lambda}; \mathbf{x}, \mathbf{y}, \mathbf{a}, \mathbf{b}) = \prod_{i=1}^N \lambda \cdot \text{lognormal}(y_i | \mu_i, \sigma_i) + (1 - \lambda) \cdot \text{truncated\_normal}(y_i | \mu_i, \sigma_i, a_i, b_i) \quad (14)$$

where  $\lambda$  controls the weighting between the two distributions. The lognormal distribution is defined as in Section 3.2.1, whereas the truncated normal distribution is defined as such:

$$\mathcal{L}(\boldsymbol{\gamma}; \mathbf{x}, \mathbf{y}) = \prod_{i=1}^N \frac{1}{\sigma\sqrt{2\pi}} \frac{\exp\left(-\frac{1}{2}\left(\frac{y_i - \mu_i}{\sigma}\right)^2\right)}{\Phi\left(\frac{b - \mu_i}{\sigma}\right) - \Phi\left(\frac{a - \mu_i}{\sigma}\right)} \quad (15)$$

The denominator accounts for proper normalization between the truncation limits because  $\Phi(\cdot)$  is simply the cumulative distribution function of the standard normal distribution, defined as follows:

$$\Phi(x) = \frac{1}{2} \left[ 1 + \text{erf}\left(\frac{x}{\sqrt{2}}\right) \right] \quad (16)$$

This model allows for better handling of uncertainty in upper limits by incorporating the possibility of them representing values near the detection limit or near the established relation, thus providing a more accurate reflection of the data.

### 3.3. Bayesian Hurdle Model

As mentioned before, the hurdle model combines both logistic and linear regressions. Thus, the expected response value ( $\log(M_\bullet)$ ) in terms of the predictor ( $\log(\sigma)$ ) is given by:

$$E[\log M_\bullet] = \left( \frac{1}{1 + e^{-(\beta_0 + \beta_1 \log \sigma)}} \right) (\gamma_0 + \gamma_1 \log \sigma) \quad (17)$$

The first term is the Bernoulli probability  $\mathbf{p}$  (see Equation (3)) of having a BH and it is dictated by the parameters  $\beta_0$  and  $\beta_1$  from the logistic regression. The second term is the linear portion of the curve and is governed by the parameters  $\gamma_0$  and  $\gamma_1$  from the linear regression (e.g. Eadie et al. 2022, Berek et al. 2023).

We used the `brm` function from the `brms` package to generate the base Stan code. The default prior distributions for the parameters are uniform (improper) distributions. To explore the impact of prior choices, we also considered weak (proper) priors on the fit parameters defined as follows:

$$\begin{aligned} \beta_0 &\sim \mathcal{N}(0, 5) \\ \beta_1 &\sim \mathcal{N}(5, 5) \\ \gamma_0 &\sim \mathcal{N}(0, 5) \\ \gamma_1 &\sim \mathcal{N}(5, 5) \end{aligned}$$

Here,  $\beta_0$  and  $\gamma_0$  are sampled from a normal distribution with a mean  $\mu = 0$  and a standard deviation  $\sigma = 5$ , while  $\beta_1$  and  $\gamma_1$  are sampled from a normal distribution with  $\mu = 5$  and  $\sigma = 5$ . Prior predictive checks demonstrated that these weak priors had a minimal impact on the model results. Despite their limited influence, we chose to use these weak priors for our analysis, as they provide slightly more informative constraints compared to uniform priors.

**Table 1.** Hurdle Model Coefficients

Parameter	Estimate	95% Credible Interval
$\beta_0$	-4.36	(-8.86, 0.17)
$\beta_1$	4.27	(1.93, 6.87)
$\gamma_0$	-4.85	(-5.30, -4.40)
$\gamma_1$	5.76	(5.56, 5.95)
$\lambda$	0.98	(0.92, 1.00)

Uncertainties are treated differently depending on the type of mass measurement, which is separated into three categories: (1) zero upper limits, (2) nonzero upper limits, and (3) precise measurements. The first is simply an upper limit quoted at  $M_\bullet = 0$ , meaning there is no evidence for the presence of a BH, whereas the second is an upper limit quoted at some  $M_\bullet > 0$ , meaning that there is evidence for a central BH with mass equal to or lower than this upper limit, but no certainty. An example of these are the low velocity dispersion galaxies from Beifiori et al. (2009) and Beifiori et al. (2012) that present evidence of a BH, but are systematically offset from the  $M_\bullet - \sigma$  relation. Thus, they are treated as nonzero upper limits. The third is a measurement for

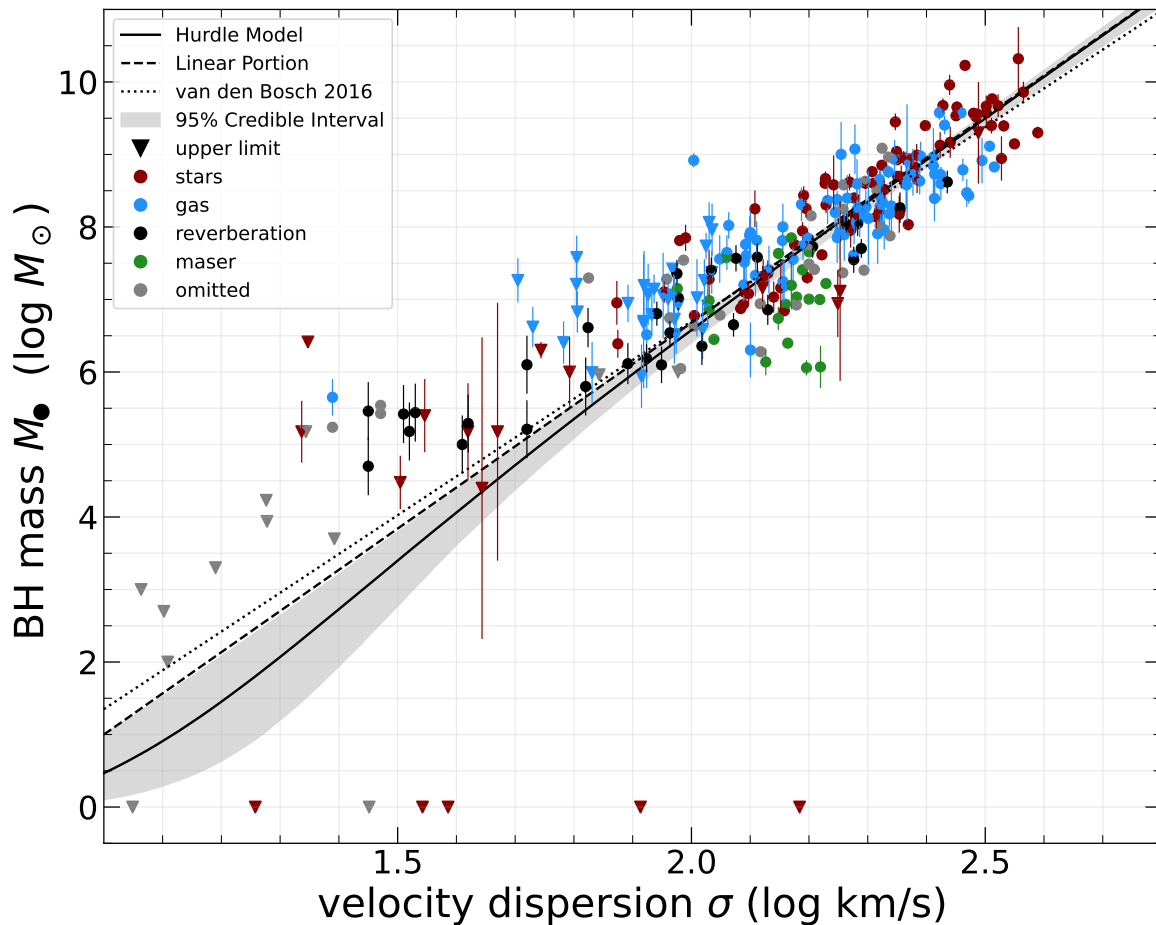


**Figure 1.** Correlation between black hole (BH) mass and stellar velocity dispersion ( $\sigma$ ). The solid black line shows the average fit obtained via our hurdle model, which includes uncertainties on the BH mass. The grey shaded region denotes the 95% Bayesian credible interval. The dashed line shows the linear portion of the fit, without considering the probability of containing a BH. The dotted black line shows the fit obtained in [van den Bosch \(2016\)](#) with an intrinsic scatter of  $\epsilon = 0.49 \pm 0.03$ . Upper limits are plotted as triangles and precise mass measurements are plotted as circles, both with their respective error bars. BH masses obtained by stellar dynamics, gas dynamics, reverberation mapping and water masers are plotted in red, blue, black and green, respectively. The BHs omitted from the fits are plotted in grey. We notice that the slope of our model’s linear portion is steeper than that of [van den Bosch \(2016\)](#).

which  $M_{\bullet} > 0$  and we are certain that there is a BH, such as NGC 1194 (e.g. [Greene et al. 2010](#), [Greene et al. 2011](#)).

The zero upper limits comprise  $\approx 2\%$  (5/244) of the sample and are treated as zeros ( $Y_i = 0$ ) in the logistic portion of our model. The nonzero upper limits represent  $\approx 18\%$  (44/244) of the dataset. In our two-step approach, they act as zeros ( $Y_i = 0$ ) for the logistic portion of the model and are modeled by the mixture model in the linear portion. Their uncertainties are passed as the scale parameter in Equation (14). The remaining  $\approx 80\%$  (i.e. 195/244) of the sample consists of precise measurements and are also treated in a two-step process. They act as ones ( $Y_i = 1$ ) for the logistic portion and have their mass measurement modeled using the lognormal

distribution in the linear portion. Their uncertainties are treated as the scale parameter  $\sigma$  in Equation (13).

When applying this model to our dataset, we obtain the mean parameter values shown in Table 1, with their respective posterior distributions in A1. The mean estimate is plotted as the solid black curve in Figure 1 by using these values and Equation (17). The 95% Bayesian credible interval is shown as the grey density plot.

We also investigated the impact of including upper limits. To achieve this, we compared the fit obtained in Figure 1 with a fit that disregards these upper limits. This alternative fit treats all data points as precise mass measurements, with the framework described in Section 3.2.1. The comparison is illustrated in Figure 2.

Appendix A presents the posterior distributions resulting from our model. In Figure A1, posterior dis-

tributions of the hurdle model parameters can be seen, whereas Figure A2 presents the posterior distributions of BH mass conditioned on several values of velocity dispersion.

## 4. DISCUSSION AND COMPARISONS

### 4.1. Previous studies

As mentioned in Section 1, there have been many studies pertaining to the  $M_{\bullet} - \sigma$  relation. One of the first was Ferrarese & Merritt (2000), in which they used the Bivariate Corrected Errors and Intrinsic Scatter (BCES) estimator from Akritas & Bershady (1996). The BCES estimator is intuitive because it is a generalization of the well-known ordinary least squares method. Thus, it takes the form of a simple regression model  $X_{2i} = \alpha + \beta X_{1i} + e_i$ , where the parameters  $\alpha$  and  $\beta$  are correlated to the moments of the bivariate distribution of  $(X_2, X_1)$  and where  $e_i$  is an error term assumed to have zero mean and finite variance (e.g. Akritas & Bershady 1996). The BCES method is useful because it accounts for measurement errors on both predictor and response variables while also allowing for these errors to be dependent (e.g. Akritas & Bershady 1996). Using this method, Ferrarese & Merritt (2000) obtain  $M_{\bullet} \propto \sigma_c^{4.8 \pm 0.5}$ , which had a flatter slope than those found by recent studies. This can be explained by the more limited data at the time, resulting in a small sample size of only 12 robust BH mass measurements. Although it should not have a considerable effect on the results, we note that they used  $\sigma_c$ , whereas we prefer to use  $\sigma_e$  when available.

Subsequently, a new fitting method introduced in Gültekin et al. (2009) was used to model the  $M_{\bullet} - \sigma$  relation. Here, a generalized MLE method that is much more complex than the BCES estimator was used. It not only includes measurement errors on both predictor and response variables, but also allows for the inclusion of upper limits on mass measurements in the model. Upper limits were included via their likelihood function which included the probability, assumed to be constant for all  $\sigma$ , that a galaxy may lack a central BH. Using a sample of 49 precise BH mass measurements and 19 upper limits, these authors found  $M_{\bullet} \propto \sigma_e^{4.2 \pm 0.4}$ .

The study by van den Bosch (2016) encompasses the most diverse measurements as it uses a large sample of 230 BH masses, resolved via several different methods, including 49 upper limits. This will be our reference for comparison as our sample is built upon theirs. They use the *mlinmixerr* and *linmixerr* routines from Kelly (2007), which operate under a Bayesian framework to perform multiple linear regression, taking the general form  $\eta_i = \alpha + \beta^T \xi_i + \epsilon_i$  (see Section 4.3 of Kelly 2007).

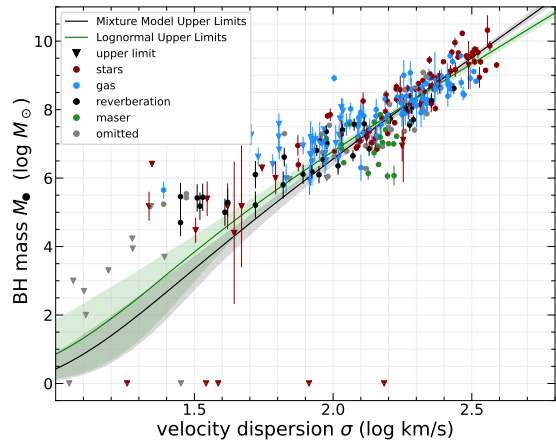


**Figure 2.** The solid black line shows the average fit obtained, along with its 95% credible interval, when treating the nonzero upper limits differently than the precise mass measurements, with a mixture model rather than a lognormal likelihood. The solid green line shows the average fit obtained, along with its 95% credible interval, when treating the nonzero upper limits in the same manner as the precise measurements, that is with a lognormal likelihood. We notice that treating the upper limits has a considerable effect, ultimately dragging the curve downwards at the low-mass end and upwards at the high-mass end.

These algorithms are powerful as they account for selection effects (e.g. Leistedt et al. 2016) and nondetections in the data sample. This is particularly useful in our case because it introduces a new way of treating the upper limits. In this method, upper limits are treated as nondetections due to observational limits rather than galaxies potentially lacking a central BH. They obtain  $M_{\bullet} \propto \sigma^{5.4 \pm 0.2}$ , which is steeper than previous studies, but can be attributed to the inclusion of a larger and more diverse sample, encompassing low-mass galaxies and upper limits, in their analysis.

Treating the upper limits is a difficult task because it heavily relies on assumptions made on the nature of these nondetections. Nevertheless, it is important to include them in the  $M_{\bullet} - \sigma$  relation as they represent a non-negligible portion of currently available data on BH masses (e.g. Boeker et al. 1999, Barth et al. 2009, Neumayer & Walcher 2012, Nguyen 2017). Some studies treat these as nondetections due to lack of precision in the measurement methods, whereas others treat them as the lack of a central BH.

In this paper, we account for both of these possibilities as there is significant observational evidence supporting the two theories, such as the case of M33 (e.g. Ferrarese & Merritt 2000, Merritt et al. 2001, Gebhardt et al. 2001). This bulgeless galaxy has a velocity dispersion of  $21 \text{ km/s} \leq \sigma_c \leq 34 \text{ km/s}$  (e.g. Merritt et al. 2001), which suggests a central BH mass of  $\approx 7000 M_{\odot}$  using



the relation from Ferrarese & Merritt (2000). In Gebhardt et al. (2001), they suggest a conservative upper limit on the mass of  $1500 M_{\odot}$ , while Merritt et al. (2001) suggests an upper limit of  $3000 M_{\odot}$ . Even if the latter is true, it still lies significantly below what is predicted. However, Gebhardt et al. (2001) show that the Hubble Space Telescope Wide Field and Planetary Camera 2 photometry and Space Telescope Imaging Spectrograph spectroscopy data are best fit by 3-integral dynamical models when the BH mass is zero, suggesting the lack of a central BH. Other studies also suggest the lack of a BH in low-mass galaxies (e.g. Greene & Ho 2007, Trump et al. 2015, Greene et al. 2020). The ambiguity surrounding whether M33 hosts a galaxy without a central BH or is simply a nondetection highlights the significance of considering both of these scenarios.

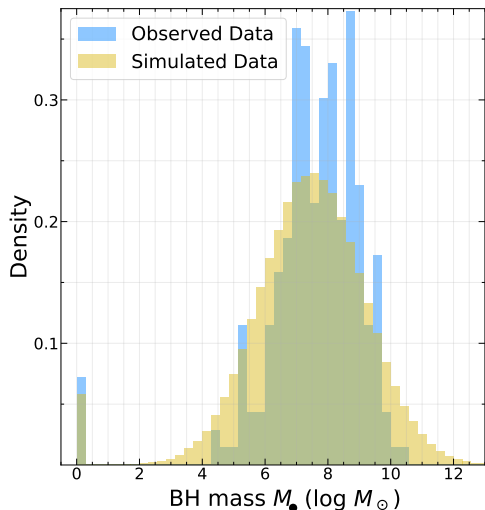


**Figure 3.** Comparison of BH mass marginal distributions between observed (blue) and simulated (yellow) data. The simulated data represents 1000 simulated points for each of the 1000 randomly chosen posterior samples. Both distributions have been normalized for comparison. Although the simulated data has much higher variance than the observed data, it manages to accurately capture the distribution of upper limits.

#### 4.2. Our results

We introduced a novel technique, previously used in Eadie et al. (2022) and Berek et al. (2023), to fit the  $M_{\bullet} - \sigma$  relation. In Eadie et al. (2022) and Berek et al. (2023), this model was used to fit the relation between the mass of a globular cluster system and its host galaxy mass. Their method allowed them to model the probability that a galaxy will contain a GC system, just as it

allows us to estimate the probability that galaxies at a certain mass (and hence velocity dispersion) will host a BH.

The adoption of weakly informative priors, as opposed to uniform priors, had a negligible effect on our results. The median values of the linear parameters remained unchanged, while the median values of the logistic parameters,  $\beta_0$  and  $\beta_1$  (see Table 1), varied by less than 1%. Similarly to Eadie et al. (2022), we opted for weakly informative priors, despite their minimal impact, particularly for  $\gamma_1$  and  $\beta_1$  because they incorporate the reasonable assumption that both parameters should be positive, given the positive nature of the underlying trends (e.g. Kormendy & Ho 2013, van den Bosch 2016).

As explained in Section 3, the hurdle model applied to our 244 objects results in a fit that is not strictly linear, but rather has a linear portion and a logistic portion. Figure 1 demonstrates how our fit deviates from the relation obtained in van den Bosch (2016). The shaded grey region represents the 95% Bayesian credible interval and is not to be mistaken with scatter. It is a density plot of the posterior samples and does not take into account the randomness of the data generating process. This results in a more tightly constrained region than usual plots of  $M_{\bullet} - \sigma$  scatter, such as in van den Bosch (2016). This also explains why the shaded region does not necessarily capture the data, especially for low velocity dispersion values. The solid black line represents the expected value or the mean of this posterior distribution. The implications of our hurdle model for the low-mass end, transition region and high-mass end will be discussed further in Sections 4.2.2, 4.2.3 and 4.2.4, respectively.

Figure 2 highlights the importance of accounting for upper limits in the analysis. It compares the fit depicted in Figure 1 with an alternative fit, in green, where upper limits are treated in the same manner as the precise measurements. The use of a mixture model in the former case drags the curve downwards, particularly at lower velocity dispersions where upper limits are more prevalent. This is the result of our model accounting for the possibility that these upper limits represent under-massive BHs or simply nondetections, thus lowering the mean BH mass for small galaxies. Consequently, the linear portion follows  $M_{\bullet} \propto \sigma^{5.8}$ , exhibiting a steeper trend compared to findings in Ferrarese & Merritt (2000), Gültekin et al. (2009) and van den Bosch (2016). The comparison with the analysis of van den Bosch (2016) is especially significant as we used a nearly identical data sample. This steepening in the linear portion is a result of our approach to incorporating the upper limits. Thus, it heavily relies on the assumption that the up-

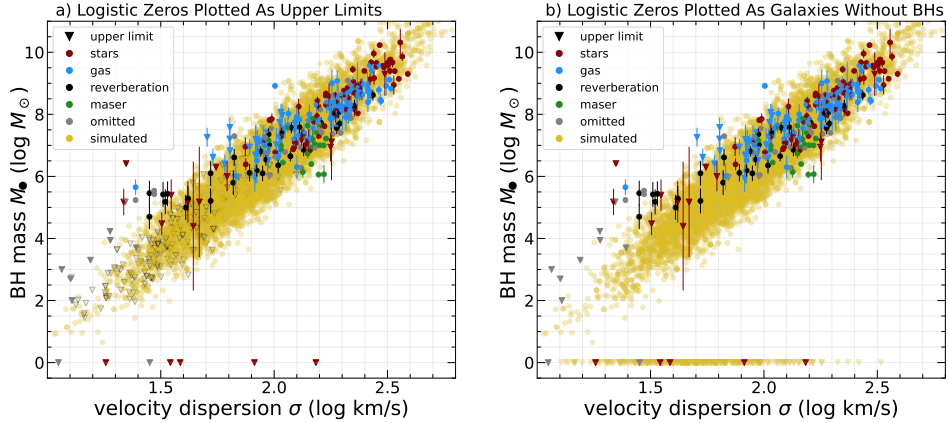


**Figure 4.** Simulated data (yellow) plotted against observational data, with two different interpretations of the logistic portion zeros: a) Treating them as upper limits, meaning galaxies that may lack a BH or are simply nondetections. b) Treating them as galaxies with no central BH. We favor the interpretation of panel a), which is more physically motivated, as discussed in Section 4.2.1.

per limits’ mass distribution is well represented by our mixture model.

The variability in velocity dispersion measurements was argued in Tremaine et al. (2002) to be an important consideration when analyzing the  $M_{\bullet} - \sigma$  relation. In our study, we prioritize  $\sigma_e$  over  $\sigma_c$ , as  $\sigma_e$  provides a more accurate representation of the three-dimensional velocity structure within the half-light radius (e.g. Gültekin et al. 2009, van den Bosch 2016). This choice is supported by the more recent findings of Gültekin et al. (2009), who argue that there is no systematic bias when comparing  $\sigma_e$  and  $\sigma_c$ . Specifically,  $\sigma_e$  is defined by integrating the contributions of both the velocity dispersion and the rotational component, weighted by the galaxy’s surface brightness (e.g. Falcón-Barroso et al. 2017). This helps to mitigate potential uncertainties arising from differences in velocity dispersion measurements across studies.

Using the logistic portion, we find that the 50%, 90% and 99% probability of hosting a central BH is attained at  $\sigma$  values greater than 11, 34 and 126 km/s, corresponding to predicted BH masses of 11.1,  $9.8 \times 10^3$  and  $1.7 \times 10^7 M_{\odot}$ , respectively. Interestingly, a velocity dispersion of 11 km/s is even smaller than that of the Small Magellanic Cloud (SMC), a nearby dwarf galaxy (e.g. Harris & Zaritsky 2006, Di Teodoro et al. 2019). At 34 km/s, we reach a velocity dispersion on the order of the Large Magellanic Cloud (LMC), another dwarf companion to our Milky Way, whereas a velocity dispersion of 126 km/s approaches that of the Milky Way itself (e.g. Bekki & Chiba 2005, Valenti et al. 2018). While the SMC has little evidence pertaining to a central BH (e.g. Lazzarini et al. 2019), Boyce et al. (2017) explore the

possibility that a galaxy as small as the LMC contains a BH.

As seen in Table 1, the logistic parameters  $\beta_0$  and  $\beta_1$  are weakly constrained, meaning the values stated in the previous paragraph are highly uncertain. This is emphasized by the wide posterior distributions of  $\beta_0$  and  $\beta_1$  in Figure A1. The nature of our dataset, which has not been corrected for selection effects, further amplifies this uncertainty (e.g. Shen et al. 2011). Not accounting for selection effects can skew our understanding of the BH occupation fraction, particularly with a heterogeneous dataset like ours (e.g. Reines & Volonteri 2015, Miller et al. 2015). This bias arises because our sample is neither volume-limited nor unbiased, leading to an overrepresentation of certain types of galaxies, especially those with more easily detectable supermassive BHs. For example, many of the galaxies in our dataset are AGNs because they are more readily detectable due to their high luminosity and distinctive emission features (e.g. Kauffmann et al. 2003a, Heckman & Best 2014). This preference for detecting AGNs contributes to the bias, as AGNs are more likely to be observed compared to inactive galaxies and necessarily harbor a central BH (e.g. Genzel et al. 2010, Greene 2012, Kormendy & Ho 2013). Consequently, this overrepresentation may inflate estimates of the probability of hosting a central BH in certain galaxy populations (e.g. Miller et al. 2015). Addressing these challenges by incorporating selection effects would necessitate a more complex approach, requiring the design of a detailed hierarchical model tailored to each type of measurement. Such an approach is beyond the scope of the current study, and therefore, we leave this for future work. Although our findings suggest that most massive galaxies, as well as

several dwarf galaxies, are likely to harbor a central BH, these results must be interpreted within the context of these limitations.

#### 4.2.1. Data Simulation

We simulated data to test our model’s predictions when simulating from a broader and more complete galaxy distribution. This involved randomly selecting 1000 posterior samples and generating 1000 data points for each sample. The simulated data’s stellar velocity dispersions were drawn randomly from the Balmer line velocity dispersion distribution of the DR8 Sloan Digital Sky Survey MPA-JHU Value-Added Catalog (VAC) (see Kauffmann et al. 2003b, Brinchmann et al. 2004, Tremonti et al. 2004, Aihara et al. 2011). We employed this approach to ensure a more exact representation of the local galaxy distribution, given the constraints of our dataset, which includes only galaxies with dynamically or temporally resolved BHs. Additionally, it enables us to capture low-mass galaxies more accurately in our simulated data, a critical consideration with the advent of upcoming 30-40m telescopes allowing us to probe their central BHs (e.g. Yelda et al. 2013, Do et al. 2014). We examined both the velocity dispersion distributions from Balmer lines and forbidden lines, sourced from the VAC. Since the distributions were nearly identical, we opted to use the one from Balmer lines, given that a portion of our data sample’s velocity dispersions originate from Balmer lines (e.g. Barth et al. 2009, Bennert et al. 2011, van den Bosch 2016). Prior to drawing the velocity dispersions, we removed outliers and used a redshift cutoff of  $z \approx 0.1$ , which corresponds to the highest redshift galaxy in our data sample. The conclusions drawn from our study are therefore only applicable to the Universe up to this redshift, where the BH mass measurements are more reliable.

We investigate the predictions of our model by comparing the BH mass marginal distributions of our observational data with our simulated data in Figure 3. Our findings reveal a decent similarity between the distributions, with the simulated data (depicted in yellow) closely mirroring the observed data (depicted in blue). The main distinctions between the two distributions lie in their spread: the observed data shows a higher peak towards the center with a narrower spread, whereas the simulated data exhibits broader tails. These variations stem from the use of a distinct velocity dispersion distribution when generating the simulated data. Remarkably, despite drawing initial velocity dispersions for simulation from the SDSS distribution, our simulated data accurately captures the distribution of upper

limits, which are prominently represented at a BH mass of zero.

To further assess the model’s predictions, we also plot simulated data against our observational data in Figure 4. Given the considerable uncertainty in the logistic parameters, we investigate two alternative interpretations of these simulated data. In the left panel, we consider the possibility that simulated zeros in the logistic portion represent upper limits, indicating galaxies that may lack a central BH or may simply be nondetections. In the right panel we explore the idea that these simulated zeros correspond to galaxies genuinely devoid of a BH. Thus, in the left panel, we plot the simulated zeros from the logistic portion as upper limits at their corresponding simulated mass from the linear portion, while in the right panel, they are represented at a BH mass of zero.

As discussed in Section 4.2, galaxies with velocity dispersions less than 34 km/s exhibit a probability of less than 10% of hosting a central BH. Consequently, we anticipate that galaxies lacking a central BH would predominantly fall below this  $\sigma$  threshold, especially seeing as most of the galaxies from the SDSS distribution have low velocity dispersions. Contrary to this expectation, under the assumption depicted in the right panel for our simulated data, a substantial majority (approximately 75%) of galaxies without a central BH possess  $\sigma \geq 33$  km/s. Furthermore, with the interpretation of the right panel, we find that approximately 2.1% of simulated data corresponds to galaxies devoid of central BHs, meanwhile they represent 0.8% of observed data. These inconsistencies prompt us to favor a more lenient interpretation of the simulated zeros, as proposed in the left panel, where they merely represent a potential absence of a central BH. This lenient interpretation also aligns well with our understanding that the BH occupation fraction is highly uncertain, due to selection effects and our biased data sample.

#### 4.2.2. Implications for the low-mass end

The low-mass end of the  $M_{\bullet} - \sigma$  relation allows us to better understand the formation of intermediate-mass BHs, which are thought to be the seeds from which supermassive BHs grow (e.g. Mezcua 2017). In Volonteri & Natarajan (2009) and Van Wassenhove et al. (2010), they suggest that the low-mass end of the relationship between BH mass and velocity dispersion flattens towards an asymptotic value if BH seeds are heavy, i.e.  $10^5 M_{\odot}$ , resulting in a distinctive “plume” of ungrown BHs. They mention that this is a signature of direct collapse models (see Begelman et al. 2006). In contrast, they show that the observable scaling rules would not detect the asymptotic value if BH seeds are light, of or-

der  $10^2 M_\odot$ , as anticipated by models akin to Population III stars (e.g. [Alighieri et al. 2008](#)). This is explained by the fact that the asymptotic value lies at masses below our observational limit.

Several observational studies have found a flattening of the curve (e.g. [Reines & Volonteri 2015](#), [Ferré-Mateu et al. 2015](#), [Mezcua 2017](#), [Martin-Navarro & Mezcua 2018](#)), supporting direct collapse models. [Reines & Volonteri \(2015\)](#) even observe this flattening in their relationship between BH mass and host galaxy total stellar mass. This was done using a sample of 262 broad-line active galactic nuclei and 79 galaxies with dynamically resolved BHs, excluding upper limits. In [Mezcua \(2017\)](#), they provide an overview of the observational evidence for intermediate-mass BHs and show that they also observe this "plume", around  $10^5 - 10^6 M_\odot$  when plotting them against the  $M_\bullet - \sigma$  relation derived in [Kormendy & Ho \(2013\)](#). They mention that this could possibly be due to observational biases, which are further discussed in [Pacucci et al. \(2018\)](#). [Pacucci et al. \(2018\)](#) simulate the coevolution of central BHs and their host galaxies using a semi-analytical model. Their results predict a deviation from the  $M_\bullet - \sigma$  relation around  $10^5 M_\odot$ , resulting in under-massive BHs. They suggest that this could be caused by the fact that smaller BHs exhibit inefficient growth and are incapable of producing substantial outflows sufficient to initiate the growth-regulation mechanism.

In a more recent study, [Greene et al. \(2020\)](#) find no evidence for a change in the  $M_\bullet - \sigma$  relation at low  $\sigma$  values, but rather a higher scatter. This results in a wider distribution of both over-massive and under-massive BHs when considering the low-mass end.

Our model predicts under-massive BHs, ranging from  $\approx 10 - 10^5 M_\odot$ , when compared to the scaling relation from [van den Bosch \(2016\)](#) for the low-mass end of the fit. This is similar to the result from the simulations in [Pacucci et al. \(2018\)](#) and further supports the theory that the flattening in the  $M_\bullet - \sigma$  relation is simply due to our limited observational capacities. This also suggests a higher number of intermediate-mass BHs and BH seeds formed by the collapse of Population III stars or via mergers in dense stellar clusters (e.g. [Mezcua 2017](#)). Although our results are in discordance with direct collapse models for the origin of seed BHs, this could be biased by our assumption that our model for the upper limits is realistic. If the true masses of these BHs are significantly closer to the upper limit, this assumption may force the low-mass end of our fit to be pulled excessively downward.

Identifying BHs in lower mass galaxies, such as the SMC and the LMC, presents unique challenges that may

contribute to the observed discrepancies in the mass estimates and their relationships with host galaxy parameters (e.g. [Lazzarini et al. 2019](#)). The irregular morphology and complex stellar dynamics of these galaxies complicate the determination of the galactic center, which is crucial for accurate measurements of key parameters needed for BH identification (e.g. [Di Teodoro et al. 2019](#)). Furthermore, the low luminosity of these systems can hinder detection, particularly when using traditional methods that rely on observing the motion of surrounding stars (e.g. [Boyce et al. 2017](#)). These difficulties emphasize the need for a careful interpretation of our findings regarding the low-end of the  $M_\bullet - \sigma$  relation.

The existence of additional under-massive BHs bodes well for the upcoming generation of giant segmented-mirror telescopes, such as the Extremely Large Telescope and the Thirty Meter Telescope. These telescopes will achieve unprecedented infrared resolution and sensitivity (e.g., [Yelda et al. 2013](#)). Their observational capacities will enable the definitive detection of galaxies hosting intermediate-mass BHs, approximately  $\sim 10^4 M_\odot$ , within the local group (e.g., [Do et al. 2014](#)). This corresponds to galaxies with velocity dispersions of 35 km/s given the linear portion and we expect 90% of them to host a central BH if our hurdle model is correct. As indicated by our simulated data in Figures 3 and 4, the number of potential candidates in this mass range is likely more extensive than previously envisioned.

#### 4.2.3. Implications for the transition region

[Martin-Navarro & Mezcua \(2018\)](#) derive the  $M_\bullet - \sigma$  relation from a sample of only low-mass galaxies. This results in a fit that overestimates the relation from [van den Bosch \(2016\)](#) until a transition mass of  $3.4 \pm 2.1 \times 10^{10} M_\odot$ , after which it underestimates it. Conversely, our model predicts under-massive BHs until a transition mass of  $\approx 1.8 \times 10^7 M_\odot$ , whereafter it predicts over-massive BHs. This discrepancy can be explained by several factors. The linear  $M_\bullet - \sigma$  relation is known to flatten at the low-mass end and [Martin-Navarro & Mezcua \(2018\)](#) use a data sample comprised of only low-mass galaxies, resulting in a flattened curve. Meanwhile, our data sample contains both low-mass and high-mass galaxies. In addition, our model takes into consideration the upper limits by treating them with a mixture model, which also tends to drag the curve downward.

#### 4.2.4. Implications for the high-mass end

When considering the high-mass end, there is a discrepancy between the  $M_\bullet - \sigma$  relation and the  $M_\bullet - L$  relation (e.g. [Lauer et al. 2007](#), [Mezcua et al. 2018b](#),



Dullo et al. 2021). The latter is an empirical correlation between central BH mass and its host galaxy’s V-band/B-band/K-band/R-band luminosity (see Faber et al. 1989, Faber et al. 1997, Merritt & Ferrarese 2001, Graham 2007). This inconsistency is thought to be due to the presence of brightest cluster galaxies (BCGs), whose stellar velocity dispersion increases weakly with luminosity although they harbor the most massive BHs (e.g. Oegerle & Hoessel 1991, Boylan-Kolchin et al. 2006, McNamara et al. 2009, Hlavacek-Larrondo et al. 2012, Mezcua et al. 2018b).

In Lauer et al. (2007), they mention that the  $M_{\bullet} - L$  relation predicts masses near  $10^{10} M_{\odot}$  for the most luminous BCGs, whereas the  $M_{\bullet} - \sigma$  relation predicts masses inferior to  $3.0 \times 10^9 M_{\odot}$ . This is also observed in Hlavacek-Larrondo et al. (2012) and Mezcua et al. (2018b). In the latter study they find that  $\approx 40\%$  of the 72 BCGs in their sample should host ultramassive BHs ( $M_{\bullet} > 10^{10} M_{\odot}$ ) if they are to be found on the FP of BH accretion (e.g. Merloni et al. 2003, van den Bosch 2016, Gültekin et al. 2019). This is of course not supported by the linear scaling relation involving stellar velocity dispersion, which underestimates these BH masses when compared to the FP detailed in Mezcua et al. (2018b).

Dullo et al. (2021) find that BH masses at the center of large-core galaxies, which make up the majority of BCGs (e.g. Laine et al. 2003), are underestimated by  $2.5 - 4\sigma_s$  when predicted by the  $M_{\bullet} - \sigma$  relation. This suggests a steepening in this linear relation when considering the high-mass end. Our results agree with this prediction when employing the hurdle model. As demonstrated in Figure 1, our fit predicts over-massive BHs for high values of  $\sigma$  ( $\gtrsim 127$  km/s) when comparing to the relation derived in van den Bosch (2016). Our hurdle model also predicts more BHs with masses greater than  $10^{10} M_{\odot}$  starting at velocity dispersion values of  $\approx 381$  km/s. Indeed, although these BHs only represent 0.8% of our observed data, they represent 6.3% of our simulated data.

The presence of ultramassive BHs at the high-mass end has several implications pertaining to our understanding of BH feedback in these host galaxies, which are most likely BCGs (e.g. Collins et al. 2009). It also has implications for the FP of BH accretion. As of now, most observational evidence shows that these BHs are positively offset from the FP of BH activity (e.g. Bontà et al. 2006, McConnell et al. 2012, Ishibashi & Fabian 2017, Mezcua et al. 2018b, Dullo et al. 2021). Mezcua et al. 2018b mention that BCGs should sit on average on the FP if they are governed by the same accretion physics as lower mass galaxies. McConnell et al. (2012) mentions that these systematic offsets allude to distinctive evolutionary mechanisms for galaxies close to clus-

ter cores. Thus, Mezcua et al. (2018b) argue against the notion of estimating BH masses in BCGs using FP correlations that favour the jet model (such as in KÖrding et al. 2006, Plotkin et al. 2012). This is supported by Dullo et al. (2021), in which they mention that such models must treat extremely massive galaxies independently. Our findings also support the existence of a  $M_{\bullet} - V_c$  correlation, where  $V_c$  is the host galaxy’s circular velocity, a proxy for dark matter halo mass. This correlation has been under debate for a long time (e.g. Volonteri et al. 2011, Bansal et al. 2022), but is supported by the presence of ultramassive BHs in BCGs (e.g. Mezcua et al. 2018b).

Furthermore, the existence of more ultramassive BHs is advantageous for the Event Horizon Telescope (EHT) as these present more candidates for imaging. Ultramassive BHs may be ideal candidates for the EHT as they have greater angular diameters (e.g. EHT Collaboration et al. 2019a). In addition, they tend to have lower angular momentum, resulting in easier targets as matter rotates the BH at lower velocities (e.g. EHT Collaboration et al. 2019a, Sisk-Reynés et al. 2022). These images are crucial as they deepen and confirm our understanding of the underlying physics of BHs (see EHT Collaboration et al. 2019a,b,c,d,e,f, 2021a,b, 2022a,b,c,d,e,f).

The two supermassive BHs imaged by the EHT are M87\* and Sagittarius A\*, which are central BHs to the host galaxies M87 and the Milky Way, respectively (e.g. EHT Collaboration et al. 2019a, Collaboration et al. 2022a). They are located at distances of 16.8 Mpc and 0.0083 Mpc while possessing respective masses of  $6.2 \times 10^9 M_{\odot}$  and  $4.1 \times 10^6 M_{\odot}$  (e.g. EHT Collaboration et al. 2019b). This results in angular diameters of  $\sim 40 \mu\text{as}$  and  $\sim 50 \mu\text{as}$ , respectively (e.g. EHT Collaboration et al. 2019d, Collaboration et al. 2022a). As an example, an ultramassive BH with  $M_{\bullet} = 10^{10} M_{\odot}$ , which is reasonable given the abundance of these ultramassive BHs in our simulated data of Figure 4, could have an angular diameter greater than  $\sim 40 \mu\text{as}$  up to a distance of  $\sim 25$  Mpc resulting in a redshift of  $z \sim 0.0059$  (e.g. EHT Collaboration et al. 2019e). BHs with masses of  $M_{\bullet} = 5 \times 10^{10} M_{\odot}$  and  $M_{\bullet} = 9 \times 10^{10} M_{\odot}$  yield the following results:  $\sim 128$  Mpc and  $z \sim 0.0305$ , as well as  $\sim 230$  Mpc and  $z \sim 0.0543$ , respectively. Thus, our findings suggest that the number of candidates for imaging by the EHT could increase significantly as ultramassive BHs up to a redshift of  $z \sim 0.0543$  may be considered.

## 5. CONCLUSION

In this paper, we apply a hurdle model to the  $M_{\bullet} - \sigma$  relation. We use a sample of 244 galaxies for which the mass of the central BH has been precisely resolved or



has been constrained to an upper limit. This hierarchical model allowed us to account for the probability that a galaxy will contain a central BH while simultaneously accounting for the relation between  $M_{\bullet}$  and  $\sigma$ . We obtain the following values for the hurdle model parameters (see Section 3.3):  $\beta_0 = -4.4$ ,  $\beta_1 = 4.3$ ,  $\gamma_0 = -4.9$ ,  $\gamma_1 = 5.8$  and  $\lambda = 0.98$ , with 95% Bayesian credible intervals of  $(-8.9, 0.2)$ ,  $(1.9, 6.9)$ ,  $(-5.3, -4.4)$ ,  $(5.6, 6.0)$  and  $(0.92, 1.00)$ , respectively.

Our findings suggest that  $M_{\bullet} \propto \sigma^{5.8}$ , by using the linear portion of our curve. This result is steeper than most studies (e.g. Ferrarese & Merritt 2000, Gültekin et al. 2009, van den Bosch 2016) and has significant effects on our understanding of galaxy and BH coevolution. It can be explained by our method of including upper limits in the analysis, as the assumption that the upper limits are well represented by our mixture model tends to steepen the curve.

Using the logistic portion of our hurdle model, we found that galaxies with  $\sigma$  values greater than 11, 34 and 126 km/s have a 50%, 90% and 99% probability of hosting a central BH. Thus, we suggest that most massive galaxies as well as many dwarf galaxies likely harbor a central BH. Although it should be noted that the previous values are highly uncertain due to the weakly constrained logistic parameters.

When comparing the hurdle model to linear models from other studies, we find that it predicts under-massive BHs, from  $10-10^5 M_{\odot}$ , when considering galaxies at the low-mass end. These results are similar to those of models related to Population III star seeds and further support the fact that the flattening in the  $M_{\bullet}-\sigma$  is due to our limited observational capacities, as discussed in Section 4.2.2 (e.g. Alighieri et al. 2008, Mezcua 2017, Pacucci et al. 2018). Though this could be biased by our assumptions on the mass distribution of the upper limits.

We also find that our fit predicts over-massive BHs when considering galaxies with high stellar velocity dispersion (i.e.  $\sigma \gtrsim 127$  km/s). This result implies the presence of more ultramassive BHs which we suggest are most likely at the center of BCGs. Hence, our results are in favor of the existence of a  $M_{\bullet}-V_c$  correlation (e.g. Mezcua et al. 2018b). We also mention that this has implications for our understanding of BH feedback in these galaxies, as they should sit on the FP of BH accretion if they are governed by the same accretion physics as lower  $\sigma$  galaxies (e.g. Mezcua et al. 2018b). Our model predicts them to be positively offset, suggesting that this is not the case (e.g. McConnell et al. 2012).

The transition between our model predicting under-massive BHs to predicting over-massive BHs happens

at  $M_{\bullet} \approx 1.8 \times 10^7 M_{\odot}$ . This is lower than the transition mass in other studies, such as Martin-Navarro & Mezcua (2018), but can be explained by the fact that we include the upper limits with a two part model, in which the logistic portion tends to drag the curve downward.

Improvements could be made to our analysis by employing more informative priors on the hurdle model parameters, as opposed to using the weak priors from Section 3.3. Although this would require extensive analysis of the galaxies with upper limits, it holds significance for the parameters in the logistic portion due to their large uncertainties. We may also consider defining a probability distribution that more accurately reflects the mass distribution of upper limits as constraints tighten, rather than relying on the assumption of our mixture model. Another improvement could involve incorporating selection effects into our Bayesian framework, following a similar approach as demonstrated in Leistedt et al. (2016). This addition could specifically target the upper limits within our dataset, distinguishing galaxies for which we are highly confident in the absence of evidence related to a central BH from those where there is only a marginal probability. The integration of such considerations into the model has the potential to better constrain the logistic portion, while also rendering this aspect of the two-step process more interpretable and less nuanced when treating upper limits.

In our study, we sought to better understand the M-sigma relation. However, when utilizing scaling relations to estimate BH masses, it is essential to consider alternative approaches that may yield more robust insights. Notably, the literature suggests that the stellar mass-BH mass relation serves as a reliable proxy across various galaxy types (e.g. Kormendy & Ho 2013, Reines & Volonteri 2015, Greene et al. 2020). While the M-sigma relation has its merits, especially in dynamically dominated systems, the correlation between stellar mass and BH mass has been well established within the context of empirical scaling relations (e.g. Ferrarese & Merritt 2000). This presents an opportunity for future studies to explore the implications of utilizing stellar mass in conjunction with our findings regarding the M-sigma relation.

## ACKNOWLEDGMENTS

J.H.-L. acknowledges support from NSERC via the Discovery grant program, as well as the Canada Research Chair program. M. M. acknowledges support from the Spanish Ministry of Science and Innovation through the project PID2021-124243NB-C22. This work was partially supported by the program Unidad de Excelencia Maria de Maeztu CEX2020-001058-M. G.M.E.

acknowledges support from NSERC via the Discovery grant program (RGPIN-2020-04554).

## DATA AVAILABILITY

All methods and data used in this paper are available at [GabrielSasseville01](#).

## APPENDIX

### A. POSTERIOR DISTRIBUTIONS

In this appendix, we present posterior distributions of interest. The posterior distributions over all hurdle model parameters are shown in Figure A1. Figure A2 shows the BH mass posterior distributions conditioned on several values of velocity dispersion, notably  $\sigma = 25$ ,  $\sigma = 50$ ,  $\sigma = 100$ ,  $\sigma = 150$ ,  $\sigma = 200$  and  $\sigma = 300$  km/s.

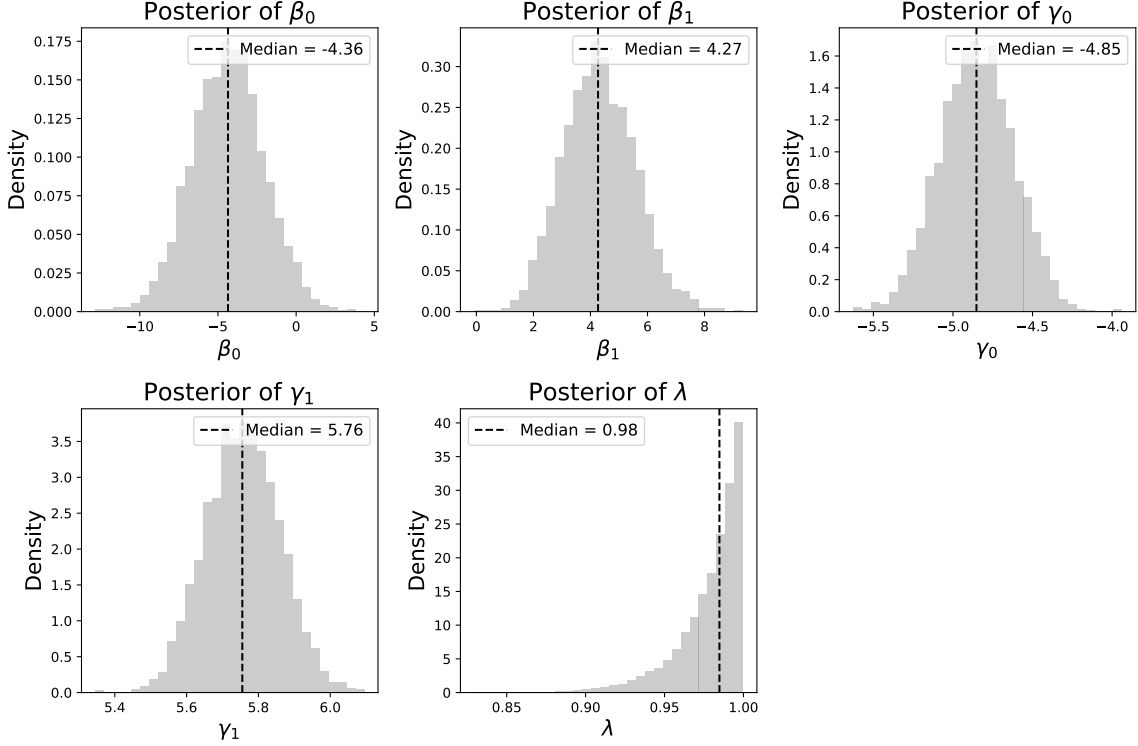


**Figure A1.** Posterior distributions of the hurdle parameters:  $\beta_0$ ,  $\beta_1$ ,  $\gamma_0$ ,  $\gamma_1$  and  $\lambda$ . The black dashed lines represent their respective median values.

### B. DATA

In this appendix, we present our data compilation. Table B1 consists of the data included in the fits, while Table B2 consists of the data excluded from the fits.

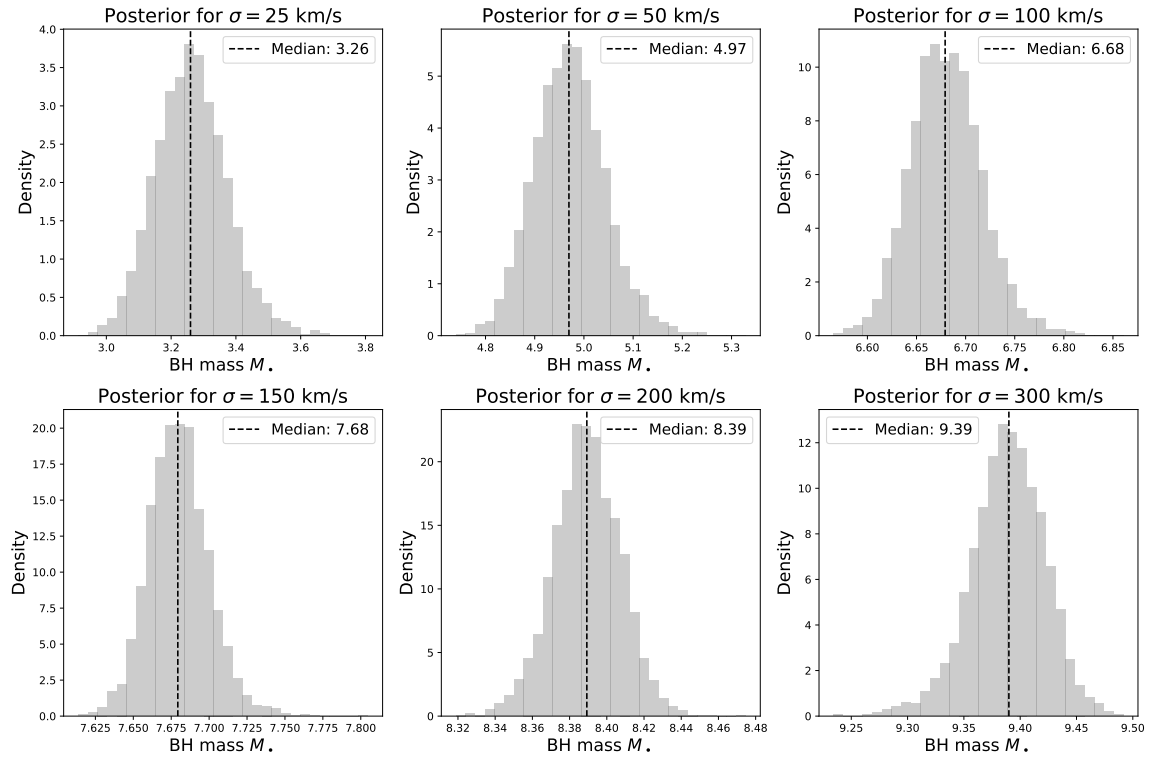


**Figure A2.** Black hole mass posterior distributions conditioned on several values of velocity dispersion:  $\sigma = 25$ ,  $\sigma = 50$ ,  $\sigma = 100$ ,  $\sigma = 150$ ,  $\sigma = 200$  and  $\sigma = 300$  km/s. The black dashed lines represent their respective median values.

Table B1. Sample of the Black Hole Mass Measurements Included in the Fits

Name	Distance (Mpc)	$M_{\bullet}$ $\log(M_{\odot})$	$\sigma_e$ $\log(\text{km s}^{-1})$	Method	$M_{\bullet}$ Uncertainty $1/2/3\sigma_s$	References
(1)	(2)	(3)	(4)	(5)	(6)	(7)
3C120	141.4±14.1	7.73±0.46	2.21±0.05	reverb	1	Kollatschny et al. (2014)
3C390.3	240.3±24.0	8.62±0.47	2.44±0.03	reverb	1	Dietrich et al. (2012)
A1836BCG	152.4±8.4	9.57±0.18	2.46±0.02	gas	1	Dalla Bontà et al. (2009)
A3565BCG	49.2±3.6	9.11±0.22	2.51±0.02	gas	1	Dalla Bontà et al. (2009)
Ark120	140.1±14.0	8.05±0.51	2.28±0.02	reverb	1	Doroshenko et al. (2008)
Arp151	90.3±9.0	6.65±0.49	2.07±0.01	reverb	1	Bentz et al. (2010)
Circinus	2.8±0.5	6.06±0.31	2.20±0.05	maser	1	Greenhill et al. (2003)
CygnusA	257.1±25.7	9.41±0.38	2.43±0.02	gas	1	Tadhunter et al. (2003)
ESO558-009	102.5±10.2	7.22±0.09	2.23±0.05	maser	1	Greene et al. (2016)
Fairall9	201.4±20.1	8.27±0.63	2.35±0.08	reverb	1	Peterson et al. (2004); van den Bosch et al. (2015)
Henize2-10	9.0±0.9	0.00 <sup>+7.00</sup> <sub>-0.00</sub>	1.54±0.19	star	3	Nguyen et al. (2014)
IC0342	3.7±0.4	6.41 <sup>+0.88</sup> <sub>-6.41</sub>	1.78±0.17	gas	1	Beifiori et al. (2012)
IC1459	28.9±3.7	9.39±0.24	2.53±0.02	star	1	Cappellari et al. (2002)
IC1481	89.9±9.0	7.15±0.40	1.98±0.12	maser	1	Huré et al. (2011); van den Bosch et al. (2015)
IC2560	41.8±4.2	7.64±0.05	2.15±0.03	maser	3	Greene et al. (2016)
IC3639	44.8±4.5	7.01 <sup>+1.06</sup> <sub>-7.01</sub>	1.96±0.02	gas	1	Beifiori et al. (2012)
J0437+2456	66.0±6.6	6.45±0.09	2.04±0.05	maser	1	Greene et al. (2016)
Mrk0050	100.3±10.0	7.40±0.53	2.03±0.06	reverb	1	Barth et al. (2011a)
Mrk0079	95.0±9.5	7.58±0.70	2.11±0.04	reverb	1	Peterson et al. (2004)
Mrk0202	90.0±9.0	6.11±0.85	1.89±0.02	reverb	1	Bentz et al. (2010)
Mrk0509	147.3±14.7	8.03±0.44	2.26±0.03	reverb	1	Peterson et al. (2004)
Mrk0590	113.0±11.3	7.55±0.54	2.28±0.01	reverb	1	Peterson et al. (2004)
Mrk0817	134.7±13.5	7.57±0.54	2.08±0.05	reverb	1	Denney et al. (2010)
Mrk1216	94.0±9.4	9.30 <sup>+2.10</sup> <sub>-6.30</sub>	2.49±0.01	star	1	Yildirim et al. (2015)
Mrk1310	83.8±8.4	6.19±0.58	1.92±0.03	reverb	1	Bentz et al. (2010)
NGC0193	49.7±5.0	8.40±0.96	2.27±0.04	gas	1	Beifiori et al. (2012)
NGC0205	0.7±0.1	0.00 <sup>+4.34</sup> <sub>-0.00</sub>	1.59±0.07	star	3	Valluri et al. (2005)
NGC0221	0.8±0.0	6.39±0.58	1.87±0.02	star	1	van den Bosch & de Zeeuw (2010)
NGC0289	17.1±1.7	7.38 <sup>+0.89</sup> <sub>-7.38</sub>	2.03±0.05	gas	1	Beifiori et al. (2012)
NGC0307	52.8±5.7	8.60±0.18	2.31±0.01	star	1	Saglia et al. (2016)
NGC0315	57.7±5.8	8.92±0.94	2.49±0.04	gas	1	Beifiori et al. (2012)
NGC0383	59.2±5.9	8.76±0.97	2.38±0.03	gas	1	Beifiori et al. (2012)
NGC0404	3.1±0.3	5.65±0.76	1.39±0.09	gas	1	Seth et al. (2010)
NGC0428	16.1±1.6	4.48 <sup>+0.37</sup> <sub>-4.48</sub>	1.50±0.07	star	3	Neumayer & Walcher (2012)
NGC0524	24.2±2.2	8.94±0.16	2.37±0.02	star	1	Krajbović et al. (2009)

Table B1 continued

Table B1 (*continued*)

Name	Distance (Mpc)	$M_{\bullet}$ $\log(M_{\odot})$	$\sigma_e$ $\log(\text{km s}^{-1})$	Method	$M_{\bullet}$ Uncertainty $1/2/3\sigma_s$	References
(1)	(2)	(3)	(4)	(5)	(6)	(7)
NGC0541	63.7±6.4	8.59±1.02	2.28±0.01	gas	1	Beifiori et al. (2012)
NGC0584	22.2±1.6	8.15±0.57	2.28±0.70	star	1	Thater et al. (2019)
NGC0598	0.8±0.1	0.00 <sup>+9.44</sup> <sub>-0.00</sub>	1.26±0.20	star	1	Gebhardt et al. (2001); Merritt & Ferrarese (2001)
NGC0613	15.4±1.5	7.60±1.05	2.09±0.07	gas	1	Beifiori et al. (2012)
NGC0741	65.7±6.6	8.67±1.11	2.37±0.02	gas	1	Beifiori et al. (2012)
NGC0788	47.9±4.8	7.92±0.84	2.10±0.06	gas	1	Beifiori et al. (2012)
NGC0821	23.4±1.8	8.22±0.63	2.32±0.02	star	1	Schulze & Gebhardt (2011)
NGC1023	10.8±0.8	7.62±0.17	2.22±0.02	star	1	Bower et al. (2001)
NGC1042	18.2±1.8	4.40 <sup>+2.08</sup> <sub>-4.40</sub>	1.64±0.07	star	3	Neumayer & Walcher (2012)
NGC1052	18.1±1.8	8.24±0.88	2.28±0.01	gas	1	Beifiori et al. (2012)
NGC1097	14.5±1.5	8.14±0.27	2.29±0.01	CO	1	Onishi et al. (2015)
NGC1194	58.0±6.3	7.85±0.15	2.17±0.07	maser	1	Kuo et al. (2011)
NGC1271	84.0±8.4	9.53±0.17	2.45±0.01	star	1	Walsh et al. (2015)
NGC1275	70.0±7.0	8.98±0.60	2.39±0.05	gas	1	Scharwächter et al. (2013); van den Bosch et al. (2015)
NGC1277	71.0±7.1	9.67±0.44	2.50±0.01	star	1	Walsh et al. (2016)
NGC1316	18.6±0.6	8.18±0.76	2.35±0.02	star	1	Nowak et al. (2008)
NGC1320	49.1±4.9	6.74±0.48	2.15±0.05	maser	1	Greene et al. (2016)
NGC1332	22.3±1.9	8.83±0.13	2.52±0.02	CO	1	Barth et al. (2016)
NGC1358	48.2±4.8	8.37±0.97	2.23±0.05	gas	1	Beifiori et al. (2012)
NGC1374	19.2±0.7	8.76±0.19	2.31±0.02	star	1	Rusli et al. (2013)
NGC1386	16.1±1.6	6.07±0.88	2.22±0.02	maser	1	Braatz et al. (1997)
NGC1398	24.8±4.1	8.03±0.25	2.37±0.01	star	1	Saglia et al. (2016)
NGC1399	20.9±0.7	8.94±0.92	2.53±0.02	star	1	Gebhardt et al. (2007); Houghton et al. (2006)
NGC1407	28.0±3.4	9.65±0.24	2.45±0.02	star	1	Rusli et al. (2013)
NGC1428	20.7±2.1	0.00 <sup>+7.00</sup> <sub>-0.00</sub>	1.91±0.02	star	3	Lyubenova et al. (2013)
NGC1493	11.4±1.1	5.40 <sup>+0.51</sup> <sub>-5.40</sub>	1.55±0.07	star	3	Neumayer & Walcher (2012)
NGC1497	75.3±7.5	8.63±0.56	2.39±0.04	gas	1	Beifiori et al. (2012)
NGC1550	51.6±5.6	9.57±0.07	2.48±0.02	star	3	Rusli et al. (2013)
NGC1600	64.0±6.4	10.23±0.12	2.47±0.02	star	1	Thomas et al. (2016)
NGC1667	56.1±5.6	8.20±0.69	2.24±0.07	gas	1	Beifiori et al. (2012)
NGC1961	48.6±4.9	8.29±1.03	2.34±0.08	gas	1	Beifiori et al. (2012)
NGC2110	29.1±2.9	8.12±1.93	2.30±0.05	gas	1	Beifiori et al. (2012)
NGC2179	35.8±3.6	8.31±0.70	2.19±0.03	gas	1	Beifiori et al. (2012)
NGC2273	29.5±1.9	6.93±0.11	2.16±0.05	maser	1	Kuo et al. (2011)
NGC2329	72.3±7.2	8.18±0.54	2.34±0.03	gas	1	Beifiori et al. (2012)
NGC2549	12.7±1.6	7.16±1.10	2.15±0.02	star	1	Krajinović et al. (2009)
NGC2685	12.5±1.3	6.59 <sup>+1.24</sup> <sub>-6.59</sub>	2.02±0.02	gas	1	Beifiori et al. (2012)
NGC2748	23.4±8.2	7.65±0.72	2.06±0.02	gas	1	Atkinson et al. (2005)

Table B1 (*continued*)



Table B1 (*continued*)

Name	Distance (Mpc)	$M_\bullet$ $\log(M_\odot)$	$\sigma_e$ $\log(\text{km s}^{-1})$	Method	$M_\bullet$ Uncertainty $1/2/3\sigma_s$	References
(1)	(2)	(3)	(4)	(5)	(6)	(7)
NGC2778	23.4±2.3	7.16 <sup>+0.91</sup> <sub>-7.16</sub>	2.12±0.02	star	1	Schulze & Gebhardt (2011)
NGC2787	7.4±1.2	7.61±0.26	2.28±0.02	gas	1	Sarzi et al. (2001)
NGC2892	86.2±8.6	8.43±0.33	2.47±0.03	gas	1	Beifiori et al. (2012)
NGC2903	10.4±1.0	7.06 <sup>+0.85</sup> <sub>-7.06</sub>	1.97±0.06	gas	1	Beifiori et al. (2012)
NGC2960	67.1±7.1	7.03±0.15	2.18±0.02	maser	1	Kuo et al. (2011); van den Bosch et al. (2015)
NGC2964	19.7±2.0	6.73 <sup>+1.84</sup> <sub>-6.73</sub>	1.97±0.09	gas	1	Beifiori et al. (2012)
NGC2974	21.5±2.4	8.23±0.27	2.36±0.02	star	1	Cappellari et al. (2008)
NGC3021	22.4±2.2	7.26 <sup>+0.91</sup> <sub>-7.26</sub>	1.70±0.20	gas	1	Beifiori et al. (2012)
NGC3031	3.6±0.1	7.81±0.39	2.15±0.02	gas	1	Devereux et al. (2003)
NGC3078	32.8±3.3	7.91±1.25	2.32±0.03	gas	1	Beifiori et al. (2012)
NGC3079	15.9±1.2	6.40±0.15	2.16±0.02	maser	1	Trotter et al. (1998); Yamauchi et al. (2004); Kondratko et al. (2005)
NGC3081	33.5±3.4	7.20±0.91	2.09±0.03	gas	1	Beifiori et al. (2012)
NGC3091	51.2±8.3	9.56±0.22	2.49±0.02	star	1	Rushi et al. (2013)
NGC3115	9.5±0.4	8.95±0.28	2.36±0.02	star	1	Emsellem et al. (1999)
NGC3227	23.8±2.6	7.32±0.70	2.12±0.04	star	1	Davies et al. (2006)
NGC3245	21.4±2.0	8.38±0.34	2.25±0.02	gas	1	Barth et al. (2001)
NGC3310	17.4±1.7	6.70 <sup>+2.77</sup> <sub>-6.70</sub>	1.92±0.02	gas	1	Pastorini et al. (2007)
NGC3351	9.3±0.9	6.52 <sup>+0.78</sup> <sub>-6.52</sub>	1.97±0.07	gas	1	Beifiori et al. (2012)
NGC3368	10.4±1.0	6.88±0.23	2.08±0.09	star	1	Nowak et al. (2010)
NGC3377	11.0±0.5	8.25±0.76	2.11±0.02	star	1	Schulze & Gebhardt (2011)
NGC3379	10.7±0.5	8.62±0.34	2.27±0.02	star	1	van den Bosch & de Zeeuw (2010)
NGC3384	11.5±0.7	7.03±0.64	2.14±0.02	star	1	Schulze & Gebhardt (2011)
NGC3393	49.2±8.2	7.20±0.99	2.17±0.03	maser	1	Kondratko et al. (2008)
NGC3414	25.2±2.7	8.40±0.21	2.28±0.02	star	1	Cappellari et al. (2008)
NGC3423	14.6±1.5	5.18 <sup>+0.67</sup> <sub>-5.18</sub>	1.62±0.07	star	3	Neumayer & Walcher (2012)
NGC3489	12.1±0.8	6.78±0.15	2.01±0.02	star	1	Nowak et al. (2010)
NGC3585	20.5±1.7	8.52±0.38	2.33±0.02	star	1	Gültekin et al. (2009)
NGC3607	22.6±1.8	8.14±0.47	2.32±0.02	star	1	Gültekin et al. (2009)
NGC3608	22.8±1.5	8.67±0.29	2.23±0.02	star	1	Schulze & Gebhardt (2011)
NGC3621	6.6±0.7	6.00 <sup>+1.43</sup> <sub>-6.00</sub>	1.79±0.03	star	1	Barth et al. (2009)
NGC3627	10.1±1.1	6.93±0.14	2.09±0.01	star	1	Saglia et al. (2016)
NGC3642	21.6±2.2	7.42 <sup>+0.12</sup> <sub>-7.42</sub>	1.97±0.11	gas	1	Beifiori et al. (2012)
NGC3665	34.7±6.7	8.76±0.27	2.34±0.02	CO	1	Onishi et al. (2016)
NGC3675	12.4±1.2	7.26 <sup>+0.88</sup> <sub>-7.26</sub>	2.02±0.02	gas	1	Beifiori et al. (2012)
NGC3706	46.0±4.6	9.77±0.18	2.51±0.01	star	1	Gültekin et al. (2014)
NGC3783	41.7±4.2	7.36±0.57	1.98±0.05	reverb	1	Onken & Peterson (2002)
NGC3801	46.3±4.6	8.28±0.93	2.32±0.04	gas	1	Beifiori et al. (2012)

Table B1 (*continued*)

Table B1 (*continued*)

Name	Distance (Mpc)	$M_{\bullet}$ $\log(M_{\odot})$	$\sigma_e$ $\log(\text{km s}^{-1})$	Method	$M_{\bullet}$ Uncertainty $1/2/3\sigma_s$	References
(1)	(2)	(3)	(4)	(5)	(6)	(7)
NGC3842	92.2±10.6	9.96±0.42	2.44±0.02	star	1	McConnell et al. (2011a)
NGC3862	84.6±8.5	8.41±1.11	2.32±0.03	gas	1	Beifiori et al. (2012)
NGC3923	20.9±2.7	9.45±0.35	2.35±0.02	star	1	Saglia et al. (2016)
NGC3945	19.5±2.0	6.94 <sup>+1.39</sup> <sub>-6.94</sub>	2.25±0.02	star	1	Gültekin et al. (2009)
NGC3953	15.4±1.5	7.33±0.87	2.11±0.01	gas	1	Beifiori et al. (2012)
NGC3982	15.9±1.6	6.95 <sup>+0.77</sup> <sub>-6.95</sub>	1.89±0.01	gas	1	Beifiori et al. (2012)
NGC3992	15.3±1.5	7.51±0.85	2.09±0.06	gas	1	Beifiori et al. (2012)
NGC3998	14.3±1.3	8.93±0.05	2.35±0.02	star	3	Walsh et al. (2012)
NGC4026	13.4±1.7	8.26±0.18	2.19±0.02	star	2	Gültekin et al. (2009)
NGC4036	19.0±1.9	7.89±1.09	2.26±0.02	gas	1	Beifiori et al. (2012)
NGC4051	10.0±1.0	6.10±0.75	1.95±0.01	reverb	1	Denney et al. (2009)
NGC4088	11.9±1.2	6.79 <sup>+0.86</sup> <sub>-6.79</sub>	1.93±0.02	gas	1	Beifiori et al. (2012)
NGC4143	14.8±1.5	7.92±1.07	2.25±0.02	gas	1	Beifiori et al. (2012)
NGC4150	12.8±1.3	5.94 <sup>+1.31</sup> <sub>-5.94</sub>	1.91±0.02	gas	1	Beifiori et al. (2012)
NGC4151	20.0±2.8	7.81±0.23	1.98±0.01	star	1	Onken et al. (2014)
NGC4203	14.1±1.4	7.82±0.78	2.11±0.02	gas	1	Beifiori et al. (2012)
NGC4212	3.2±0.3	5.99 <sup>+1.27</sup> <sub>-5.99</sub>	1.83±0.02	gas	1	Beifiori et al. (2012)
NGC4245	14.6±1.5	7.19 <sup>+1.43</sup> <sub>-7.19</sub>	1.92±0.02	gas	1	Beifiori et al. (2012)
NGC4253	55.4±5.5	6.80±0.50	1.94±0.16	reverb	1	Bentz et al. (2010)
NGC4258	7.3±0.5	7.58±0.09	2.06±0.04	maser	1	Herrnstein et al. (2005)
NGC4261	32.4±2.8	8.72±0.29	2.42±0.02	gas	1	Ferrarese et al. (1996)
NGC4278	15.0±1.5	7.96±0.81	2.33±0.02	gas	1	Beifiori et al. (2012)
NGC4291	26.6±3.9	8.99±0.47	2.38±0.02	star	1	Schulze & Gebhardt (2011)
NGC4303	17.9±1.8	6.51±2.21	1.92±0.02	gas	1	Pastorini et al. (2007)
NGC4314	15.5±1.5	6.91 <sup>+0.89</sup> <sub>-6.91</sub>	2.03±0.01	gas	1	Beifiori et al. (2012)
NGC4321	14.2±1.4	6.67 <sup>+0.50</sup> <sub>-6.67</sub>	1.92±0.02	gas	1	Beifiori et al. (2012)
NGC4335	59.1±5.9	8.39±0.94	2.41±0.01	gas	1	Beifiori et al. (2012)
NGC4342	22.9±1.4	8.66±0.56	2.38±0.02	star	1	Gretton & van den Bosch (1999)
NGC4350	17.0±1.7	8.58±1.22	2.24±0.02	star	1	Pignatelli et al. (2001)
NGC4371	16.9±1.5	6.84±0.22	2.16±0.02	star	1	Saglia et al. (2016)
NGC4374	18.5±0.6	8.97±0.14	2.41±0.02	gas	1	Walsh et al. (2010)
NGC4382	17.9±1.8	7.11 <sup>+3.71</sup> <sub>-7.11</sub>	2.25±0.02	star	1	Gültekin et al. (2011)
NGC4388	16.5±1.6	6.86±0.13	2.03±0.03	maser	1	Kuo et al. (2011)
NGC4429	18.2±1.8	7.85±1.05	2.25±0.02	gas	1	Beifiori et al. (2012)
NGC4434	20.8±1.5	7.85±0.54	1.99±1.04	star	1	Graham & Soria (2018)
NGC4435	17.0±1.7	0.00 <sup>+6.30</sup> <sub>-0.00</sub>	2.18±0.02	star	3	Coccatto et al. (2006)
NGC4450	28.3±2.8	8.06 <sup>+0.84</sup> <sub>-8.06</sub>	2.03±0.06	gas	1	Beifiori et al. (2012)

Table B1 (*continued*)

Table B1 (*continued*)

Name	Distance (Mpc)	$M_\bullet$ $\log(M_\odot)$	$\sigma_e$ $\log(\text{km s}^{-1})$	Method	$M_\bullet$ Uncertainty $1/2/3\sigma_s$	References
(1)	(2)	(3)	(4)	(5)	(6)	(7)
NGC4459	16.0±0.5	7.84±0.26	2.20±0.02	gas	1	Sarzi et al. (2001)
NGC4472	17.1±0.6	9.40±0.11	2.40±0.02	star	1	Rusli et al. (2013)
NGC4473	15.2±0.5	7.95±0.72	2.27±0.02	star	1	Schulze & Gebhardt (2011)
NGC4477	20.8±2.1	7.55±0.89	2.17±0.02	gas	1	Beifiori et al. (2012)
NGC4486	16.7±0.6	9.58±0.29	2.42±0.02	gas	1	Walsh et al. (2013)
NGC4486A	16.0±0.5	7.10±0.44	2.09±0.02	star	1	Nowak et al. (2007)
NGC4486B	16.5±0.6	8.60±0.07	2.23±0.02	star	1	Saglia et al. (2016)
NGC4501	16.5±1.1	7.30±0.24	2.20±0.01	star	1	Saglia et al. (2016)
NGC4507	47.0±4.7	7.18±1.05	2.16±0.02	gas	1	Beifiori et al. (2012)
NGC4526	16.4±1.8	8.65±0.37	2.32±0.02	gas	1	Davis et al. (2013)
NGC4548	17.9±1.8	7.25±0.88	2.16±0.04	gas	1	Beifiori et al. (2012)
NGC4552	15.3±1.0	8.70±0.15	2.35±0.02	star	1	Cappellari et al. (2008)
NGC4564	15.9±0.5	7.95±0.37	2.19±0.02	star	1	Schulze & Gebhardt (2011)
NGC4578	38.7±2.7	7.28±1.23	2.03±0.95	star	1	Graham & Soria (2018)
NGC4579	23.0±2.3	7.96 <sup>+1.08</sup> <sub>-7.96</sub>	2.04±0.06	gas	1	Beifiori et al. (2012)
NGC4593	38.5±3.9	6.86±0.62	2.13±0.02	reverb	1	Barth et al. (2013)
NGC4594	9.9±0.8	8.82±0.14	2.38±0.02	star	1	Jardel et al. (2011)
NGC4596	16.5±6.2	7.89±0.78	2.10±0.02	gas	1	Sarzi et al. (2001)
NGC4621	18.3±3.0	8.60±0.26	2.30±0.02	star	1	Cappellari et al. (2008)
NGC4649	16.5±0.6	9.67±0.30	2.43±0.02	star	1	Shen & Gebhardt (2010)
NGC4697	12.5±0.4	8.31±0.34	2.23±0.02	star	1	Schulze & Gebhardt (2011)
NGC4698	16.4±1.6	7.76±0.48	2.09±0.03	gas	1	Beifiori et al. (2012)
NGC4742	15.7±1.6	7.10±0.45	1.95±0.02	star	1	Tremaine et al. (2002)
NGC4748	62.7±6.3	6.36±0.78	2.02±0.05	reverb	1	Bentz et al. (2010)
NGC4751	26.9±2.9	9.15±0.17	2.55±0.02	star	1	Rusli et al. (2013)
NGC4762	19.2±1.4	7.36±0.54	2.13±0.95	star	1	Graham & Soria (2018)
NGC4800	12.5±1.3	7.02 <sup>+1.60</sup> <sub>-7.02</sub>	2.01±0.01	gas	1	Beifiori et al. (2012)
NGC4889	102.0±5.2	10.32±1.31	2.56±0.02	star	1	McConnell et al. (2011a)
NGC4945	3.7±0.4	6.14±0.55	2.13±0.02	maser	1	Greenhill et al. (1997)
NGC5005	14.6±1.5	8.27±0.70	2.30±0.02	gas	1	Beifiori et al. (2012)
NGC5055	8.7±0.9	8.92±0.30	2.00±0.02	gas	1	Blais-Ouellette et al. (2004)
NGC5077	38.7±8.4	8.93±0.80	2.35±0.02	gas	1	de Francesco et al. (2008)
NGC5127	62.5±6.3	8.27±1.24	2.29±0.11	gas	1	Beifiori et al. (2012)
NGC5128	3.6±0.2	7.76±0.25	2.18±0.02	star	1	Cappellari et al. (2009)
NGC5248	17.9±1.8	6.30±1.14	2.10±0.04	gas	1	Beifiori et al. (2012)
NGC5252	103.7±10.4	9.07±1.02	2.28±0.02	gas	1	Capetti et al. (2005)
NGC5273	15.5±1.5	6.61±0.81	1.82±0.02	reverb	1	Bentz et al. (2014); van den Bosch et al. (2015)
NGC5283	34.5±3.5	7.41±0.99	2.13±0.04	gas	1	Beifiori et al. (2012)

Table B1 (*continued*)

Table B1 (*continued*)

Name	Distance (Mpc)	$M_{\bullet}$ $\log(M_{\odot})$	$\sigma_e$ $\log(\text{km s}^{-1})$	Method	$M_{\bullet}$ Uncertainty $1/2/3\sigma_s$	References
(1)	(2)	(3)	(4)	(5)	(6)	(7)
NGC5328	64.1±7.0	9.67±0.16	2.52±0.02	star	3	Rusli et al. (2013)
NGC5347	32.3±3.2	7.21 <sup>+1.27</sup> <sub>-7.21</sub>	1.80±0.08	gas	1	Beifiori et al. (2012)
NGC5419	56.2±6.1	9.86±0.43	2.57±0.01	star	1	Saglia et al. (2016)
NGC5427	36.3±3.6	7.58 <sup>+0.90</sup> <sub>-7.58</sub>	1.80±0.08	gas	1	Beifiori et al. (2012)
NGC5457	7.0±0.7	6.41 <sup>+0.23</sup> <sub>-6.41</sub>	1.35±0.17	star	1	Kormendy et al. (2010)
NGC5490	65.2±6.5	8.73±1.05	2.41±0.04	gas	1	Beifiori et al. (2012)
NGC5495	126.3±11.6	7.00±0.15	2.22±0.05	maser	1	Greene et al. (2016)
NGC5516	58.4±6.3	9.52±0.17	2.48±0.04	star	1	Rusli et al. (2013)
NGC5548	73.6±7.4	7.70±0.39	2.29±0.03	reverb	1	Kovačević et al. (2014)
NGC5576	25.7±1.7	8.44±0.38	2.19±0.02	star	1	Gültekin et al. (2009)
NGC5643	17.4±1.7	7.05 <sup>+1.77</sup> <sub>-7.05</sub>	1.95±0.01	gas	1	Beifiori et al. (2012)
NGC5695	54.6±5.5	8.00±0.96	2.16±0.01	gas	1	Beifiori et al. (2012)
NGC5728	37.6±3.8	8.05±0.87	2.28±0.09	gas	1	Beifiori et al. (2012)
NGC5765B	113.0±11.3	7.66±0.09	2.20±0.05	maser	1	Gao et al. (2016)
NGC5813	32.2±2.7	8.85±0.17	2.32±0.02	star	1	Cappellari et al. (2008)
NGC5845	25.9±4.1	8.69±0.47	2.36±0.02	star	1	Schulze & Gebhardt (2011)
NGC5846	24.9±2.3	9.04±0.17	2.35±0.02	star	1	Cappellari et al. (2008)
NGC5879	10.6±1.1	6.62 <sup>+0.83</sup> <sub>-6.62</sub>	1.73±0.06	gas	1	Beifiori et al. (2012)
NGC5921	20.5±2.0	7.07 <sup>+1.27</sup> <sub>-7.07</sub>	1.93±0.05	gas	1	Beifiori et al. (2012)
NGC6086	138.0±11.5	9.57±0.50	2.50±0.02	star	1	McConnell et al. (2011b)
NGC6240(S)	105.0±10.5	9.17±0.64	2.44±0.07	star	1	Medling et al. (2011)
NGC6251	108.4±9.0	8.79±0.47	2.46±0.02	gas	1	Ferrarese & Ford (1999)
NGC6300	14.2±1.4	7.14 <sup>+0.60</sup> <sub>-7.14</sub>	1.94±0.02	gas	1	Beifiori et al. (2012)
NGC6323	113.4±12.3	7.00±0.14	2.20±0.07	maser	1	Kuo et al. (2011)
NGC6500	36.5±3.6	8.34±0.78	2.33±0.01	gas	1	Beifiori et al. (2012)
NGC6503	5.3±0.5	6.30 <sup>+0.34</sup> <sub>-6.30</sub>	1.74±0.02	star	1	Kormendy et al. (2010)
NGC6814	22.3±2.2	7.02±0.51	1.98±0.01	reverb	1	Bentz et al. (2010)
NGC6861	27.3±4.5	9.30±0.25	2.59±0.02	star	1	Rusli et al. (2013)
NGC6951	16.0±1.6	6.93 <sup>+0.56</sup> <sub>-6.93</sub>	1.98±0.04	gas	1	Beifiori et al. (2012)
NGC7052	70.4±8.4	8.60±0.69	2.42±0.02	gas	1	van der Marel & van den Bosch (1998)
NGC7331	12.2±1.2	8.02±0.55	2.06±0.02	gas	1	Beifiori et al. (2012)
NGC7332	21.7±2.2	7.08±0.53	2.10±0.02	star	1	Häring & Rix (2004)
NGC7418	18.4±1.8	5.18 <sup>+1.78</sup> <sub>-5.18</sub>	1.67±0.06	star	3	Neumayer & Walcher (2012)
NGC7424	10.9±1.1	5.18 <sup>+0.43</sup> <sub>-5.18</sub>	1.34±0.05	star	3	Neumayer & Walcher (2012)
NGC7457	12.5±1.2	6.95±0.91	1.87±0.02	star	1	Schulze & Gebhardt (2011)
NGC7582	22.3±9.8	7.74±0.61	2.19±0.05	gas	1	Wold et al. (2006)
NGC7619	51.5±7.4	9.40±0.32	2.51±0.02	star	1	Rusli et al. (2013)

Table B1 (*continued*)

Table B1 (*continued*)

Name	Distance (Mpc)	$M_\bullet$ $\log(M_\odot)$	$\sigma_e$ $\log(\text{km s}^{-1})$	Method	$M_\bullet$ Uncertainty $1/2/3\sigma_s$	References
(1)	(2)	(3)	(4)	(5)	(6)	(7)
NGC7626	38.1±3.8	8.58±0.98	2.37±0.02	gas	1	Beifiori et al. (2012)
NGC7682	59.3±5.9	7.56±0.98	2.05±0.06	gas	1	Beifiori et al. (2012)
NGC7768	116.0±27.5	9.13±0.54	2.42±0.02	star	1	McConnell et al. (2012)
NSA10779	208.2±14.6	5.44±1.20	1.53±0.78	reverb	1	Baldassare et al. (2020)
NSA125318	147.4±10.3	5.00±1.20	1.61±0.78	reverb	1	Baldassare et al. (2020)
NSA15235	135.3±9.5	5.29±1.20	1.62±1.15	reverb	1	Baldassare et al. (2020)
NSA166155	109.8±7.7	4.70±1.20	1.45±1.05	reverb	1	Baldassare et al. (2015)
NSA18913	176.9±12.4	5.18±1.20	1.52±1.15	reverb	1	Baldassare et al. (2020)
NSA47066	184.3±12.9	5.42±1.20	1.51±0.70	reverb	1	Baldassare et al. (2020)
NSA52675	70.2±4.9	6.10±1.20	1.72±0.70	reverb	1	Baldassare et al. (2020)
NSA62996	199.9±14.0	5.80±1.20	1.82±0.48	reverb	1	Baldassare et al. (2020)
NSA79874	172.2±12.1	5.46±1.20	1.45±0.85	reverb	1	Baldassare et al. (2016)
NSA99052	141.2±9.9	5.21±1.20	1.72±0.70	reverb	1	Baldassare et al. (2020)
SBS1116+583A	119.4±11.9	6.54±0.59	1.96±0.02	reverb	1	Bentz et al. (2010)
UGC12064	34.7±6.7	8.84±1.56	2.41±0.03	gas	1	Beifiori et al. (2012)
UGC1214	59.9±6.0	7.74 <sup>+0.54</sup> <sub>-7.74</sub>	2.02±0.06	gas	1	Beifiori et al. (2012)
UGC1395	60.8±6.1	6.83 <sup>+0.85</sup> <sub>-6.83</sub>	1.81±0.04	gas	1	Beifiori et al. (2012)
UGC1841	74.9±7.5	8.47±0.58	2.47±0.04	gas	1	Beifiori et al. (2012)
UGC3789	49.9±5.4	6.99±0.26	2.03±0.05	maser	1	Kuo et al. (2011)
UGC6093	150.0±15.0	7.41±0.06	2.19±0.05	maser	1	Greene et al. (2016)
UGC7115	88.2±8.8	9.00±1.34	2.25±0.08	gas	1	Beifiori et al. (2012)
UGC9799	151.1±15.1	8.89 <sup>+2.41</sup> <sub>-8.89</sub>	2.37±0.02	gas	1	Dalla Bontà et al. (2009)

NOTE—(1) Name. (2) Distance. (3) BH mass. (4) Effective stellar velocity dispersion. (5) Method used for BH mass measurement. BH masses measured using stellar dynamics, gas dynamics, reverberation mapping and water masers are denoted by keywords star, gas, reverb, maser, respectively. (6)  $1\sigma_s$ ,  $2\sigma_s$  or  $3\sigma_s$  confidence level on  $M_\bullet$  uncertainty. (7) Literature reference.



Table B2. Sample of the Black Hole Mass Measurements Excluded from the Fits

Name	Distance (Mpc)	$M_{\bullet}$ $\log(M_{\odot})$	$\sigma_e$ $\log(\text{km s}^{-1})$	Method	$M_{\bullet}$ Uncertainty $1/2/3\sigma_s$	References
(1)	(2)	(3)	(4)	(5)	(6)	(7)
1RXSJ1858+4850	338.3±33.8	6.68±0.56	-1234.00±1234.00	reverb	1	Pei et al. (2014)
G1	0.7±0.1	5.24±0.37	1.39±0.09	GC	1	Gebhardt et al. (2005)
H0507+164	76.6±7.7	6.69±1.09	-1234.00±1234.00	reverb	1	Stalin et al. (2011)
M60UCD1	16.5±1.6	7.30±0.45	1.82±0.03	star	1	Seth et al. (2014)
Mrk0006	80.6±8.1	8.09±0.46	-1234.00±1234.00	reverb	1	Doroshenko et al. (2012)
Mrk0110	151.1±15.1	7.28±0.64	1.96±0.03	reverb	1	Peterson et al. (2004)
Mrk0142	192.5±19.2	6.27±0.63	-1234.00±1234.00	reverb	1	Du et al. (2014)
Mrk0279	130.4±13.0	7.40±0.69	2.29±0.03	reverb	1	Peterson et al. (2004)
Mrk0290	126.7±12.7	7.26±0.52	-1234.00±1234.00	reverb	1	Denney et al. (2010)
Mrk0335	110.5±11.0	7.21±0.47	-1234.00±1234.00	reverb	1	Du et al. (2014)
Mrk1029	124.0±12.4	6.28±0.39	2.12±0.05	maser	3	Greene et al. (2016)
Mrk1501	382.6±38.3	8.03±0.77	-1234.00±1234.00	reverb	1	Grier et al. (2012)
MW	0.0±0.0	6.63±0.14	2.00±0.09	star	1	Ghez et al. (2008); Gillessen et al. (2009)
NGC0104	0.0±0.0	3.00 <sup>+0.53</sup> <sub>-3.00</sub>	1.06±0.03	GC	1	McLaughlin et al. (2006)
NGC0224	0.8±0.0	8.15±0.48	2.20±0.02	star	3	Bender et al. (2005)
NGC0300	2.2±0.2	2.00 <sup>+3.00</sup> <sub>-2.00</sub>	1.11±0.07	star	1	Neumayer & Walcher (2012)
NGC1068	15.9±9.4	6.92±0.74	2.18±0.02	maser	1	Lodato & Bertin (2003)
NGC1300	21.5±9.4	7.88±1.03	2.34±0.02	gas	1	Atkinson et al. (2005)
NGC1851	0.0±0.0	0.00 <sup>+3.30</sup> <sub>-0.00</sub>	0.97±0.02	GC	1	Lützgendorf et al. (2013)
NGC1904	0.0±0.0	3.48 <sup>+0.12</sup> <sub>-3.48</sub>	0.90±0.03	GC	1	Lützgendorf et al. (2013)
NGC2139	23.6±2.4	5.18 <sup>+0.43</sup> <sub>-5.18</sub>	1.34±0.08	star	1	Neumayer & Walcher (2012)
NGC2911	43.5±4.3	9.09±0.88	2.32±0.03	gas	1	Beifiori et al. (2012)
NGC3227	23.8±2.6	6.75±0.21	1.96±0.03	reverb	1	Denney et al. (2010)
NGC3516	37.9±3.8	7.37±0.16	2.26±0.01	reverb	1	Denney et al. (2010)
NGC4041	19.5±2.0	6.00 <sup>+0.61</sup> <sub>-6.00</sub>	1.98±0.02	gas	1	Marconi et al. (2003)
NGC4151	20.0±2.8	7.54±0.49	1.99±0.01	reverb	1	Bentz et al. (2006)
NGC4244	4.4±0.4	0.00 <sup>+5.66</sup> <sub>-0.00</sub>	1.45±0.15	star	3	De Lorenzi et al. (2013)
NGC4395	4.4±0.4	5.43±0.75	1.47±0.07	reverb	1	Peterson et al. (2005)
NGC4395	4.4±0.4	5.54±1.62	1.47±0.07	gas	1	den Brok et al. (2015)
NGC4636	13.7±1.4	8.58±0.66	2.26±0.02	gas	1	Beifiori et al. (2012)
NGC4699	18.9±2.1	8.25±0.16	2.26±0.01	star	1	Saglia et al. (2016)
NGC4736	4.5±0.8	6.78±0.37	2.05±0.02	star	1	Kormendy et al. (2011)
NGC4826	5.2±1.2	6.05±0.39	1.98±0.02	star	1	Kormendy et al. (2011)
NGC5018	40.5±4.9	8.02±0.23	2.32±0.01	star	3	Saglia et al. (2016)
NGC5139	0.0±0.0	3.94 <sup>+0.42</sup> <sub>-3.94</sub>	1.28±0.03	GC	1	van der Marel & Anderson (2010)

Table B2 continued

Table B2 (continued)

Name	Distance (Mpc)	$M_{\bullet}$ $\log(M_{\odot})$	$\sigma_e$ $\log(\text{km s}^{-1})$	Method	$M_{\bullet}$ Uncertainty $1/2/3\sigma_s$	References
(1)	(2)	(3)	(4)	(5)	(6)	(7)
NGC5194	$7.9 \pm 0.8$	$5.96^{+1.08}_{-5.96}$	$1.84 \pm 0.06$	gas	1	Beifiori et al. (2012)
NGC5272	$0.0 \pm 0.0$	$0.00^{+3.72}_{-0.00}$	$0.73 \pm 0.08$	GC	1	Kammann et al. (2014)
NGC5694	$0.0 \pm 0.0$	$0.00^{+3.90}_{-0.00}$	$0.94 \pm 0.03$	GC	1	Lützgendorf et al. (2013)
NGC5793	$53.3 \pm 5.3$	$7.30 \pm 7.30$	$-1234.00 \pm 1234.00$	maser	1	Hagiwara et al. (2001)
NGC5824	$0.0 \pm 0.0$	$0.00^{+3.78}_{-0.00}$	$1.05 \pm 0.02$	GC	1	Lützgendorf et al. (2013)
NGC6093	$0.0 \pm 0.0$	$0.00^{+2.90}_{-0.00}$	$0.97 \pm 0.01$	GC	1	Lützgendorf et al. (2013)
NGC6205	$0.0 \pm 0.0$	$0.00^{+3.93}_{-0.00}$	$0.85 \pm 0.06$	GC	1	Kammann et al. (2014)
NGC6264	$147.6 \pm 16.0$	$7.49 \pm 0.14$	$2.20 \pm 0.04$	maser	1	Kuo et al. (2011)
NGC6266	$0.0 \pm 0.0$	$3.30^{+0.18}_{-3.30}$	$1.19 \pm 0.01$	GC	3	Lützgendorf et al. (2013); McNamara & Nulsen (2012)
NGC6341	$0.0 \pm 0.0$	$0.00^{+2.99}_{-0.00}$	$0.77 \pm 0.07$	GC	1	Kammann et al. (2014)
NGC6388	$0.0 \pm 0.0$	$4.23^{+0.55}_{-4.23}$	$1.28 \pm 0.01$	GC	1	Lützgendorf et al. (2011)
NGC6397	$0.0 \pm 0.0$	$2.78^{+0.37}_{-2.78}$	$0.69 \pm 0.09$	GC	1	Kammann et al. (2016)
NGC7078	$0.0 \pm 0.0$	$2.70^{+2.53}_{-2.70}$	$1.10 \pm 0.20$	GC	1	van den Bosch et al. (2006); den Brok et al. (2014)
NGC7469	$47.7 \pm 8.1$	$6.94 \pm 0.16$	$2.12 \pm 0.02$	reverb	1	Peterson et al. (2014)
NGC7793	$3.3 \pm 0.3$	$3.70^{+2.20}_{-3.70}$	$1.39 \pm 0.07$	star	1	Neumayer & Walcher (2012)
PG0026+129	$608.2 \pm 60.8$	$8.46 \pm 0.66$	$-1234.00 \pm 1234.00$	reverb	1	Peterson et al. (2004)
PG0052+251	$661.5 \pm 66.1$	$8.44 \pm 0.61$	$-1234.00 \pm 1234.00$	reverb	1	Peterson et al. (2004)
PG0804+761	$428.3 \pm 42.8$	$8.72 \pm 0.16$	$-1234.00 \pm 1234.00$	reverb	1	Peterson et al. (2004)
PG0953+414	$1002.6 \pm 100.3$	$8.31 \pm 0.62$	$-1234.00 \pm 1234.00$	reverb	1	Peterson et al. (2004)
PG1226+023	$678.1 \pm 67.8$	$8.81 \pm 0.63$	$-1234.00 \pm 1234.00$	reverb	1	Peterson et al. (2004)
PG1229+204	$269.9 \pm 27.0$	$7.72 \pm 0.93$	$2.20 \pm 0.09$	reverb	1	Peterson et al. (2004)
PG1307+085	$663.8 \pm 66.4$	$8.49 \pm 0.72$	$-1234.00 \pm 1234.00$	reverb	1	Peterson et al. (2004)
PG1411+442	$383.7 \pm 38.4$	$8.50 \pm 0.78$	$2.32 \pm 0.06$	reverb	1	Peterson et al. (2004)
PG1426+015	$370.8 \pm 37.1$	$8.96 \pm 0.25$	$2.34 \pm 0.03$	reverb	1	Peterson et al. (2004)
PG1613+658	$552.5 \pm 55.2$	$8.27 \pm 0.33$	$-1234.00 \pm 1234.00$	reverb	3	Peterson et al. (2004)
PG1617+175	$481.6 \pm 48.2$	$8.63 \pm 0.66$	$2.30 \pm 0.08$	reverb	3	Peterson et al. (2004)
PG1700+518	$1250.6 \pm 125.1$	$8.76 \pm 0.63$	$-1234.00 \pm 1234.00$	reverb	1	Peterson et al. (2004)
PG2130+099	$269.7 \pm 27.0$	$7.41 \pm 0.52$	$2.21 \pm 0.05$	reverb	3	Grier et al. (2012)
Zw229-015	$119.4 \pm 11.9$	$6.88 \pm 0.63$	$-1234.00 \pm 1234.00$	reverb	1	Barth et al. (2011b)

NOTE—(1) Name. (2) Distance. (3) BH mass. (4) Effective stellar velocity dispersion. (5) Method used for BH mass measurement. BH masses measured using stellar dynamics, gas dynamics, reverberation mapping and water masers are denoted by keywords star, gas, reverb, maser, respectively. (6)  $1\sigma_s$ ,  $2\sigma_s$  or  $3\sigma_s$  confidence level on  $M_{\bullet}$  uncertainty. (7) Literature reference. It is worth noting that ... corresponds to missing data in the literature.

## REFERENCES

- Aihara, H., Allende Prieto, C., An, D., et al. 2011, *The Astrophysical Journal Supplement Series*, 193, 29, doi: [10.1088/0067-0049/193/2/29](https://doi.org/10.1088/0067-0049/193/2/29)
- Akritas, M. G., & Bershady, M. A. 1996, *The Astrophysical Journal*, 470, 706, doi: [10.1086/177901](https://doi.org/10.1086/177901)
- Albert, J. 2009, *Bayesian Computation with R* (New York, NY: Springer), doi: [10.1007/978-0-387-92298-0](https://doi.org/10.1007/978-0-387-92298-0)
- Alighieri, S. d. S., Kurk, J., Ciardi, B., et al. 2008, *Proceedings of the International Astronomical Union*, 4, 75, doi: [10.1017/S1743921308024605](https://doi.org/10.1017/S1743921308024605)
- Atkinson, J. W., Collett, J. L., Marconi, A., et al. 2005, *MNRAS*, 359, 504, doi: [10.1111/j.1365-2966.2005.08904.x](https://doi.org/10.1111/j.1365-2966.2005.08904.x)
- Baldassare, V. F., Dickey, C., Geha, M., & Reines, A. E. 2020, *The Astrophysical Journal*, 898, L3, doi: [10.3847/2041-8213/aba0c1](https://doi.org/10.3847/2041-8213/aba0c1)
- Baldassare, V. F., Reines, A. E., Gallo, E., & Greene, J. E. 2015, *ApJL*, 809, L14, doi: [10.1088/2041-8205/809/1/L14](https://doi.org/10.1088/2041-8205/809/1/L14)
- Baldassare, V. F., Reines, A. E., Gallo, E., et al. 2016, *The Astrophysical Journal*, 829, 57, doi: [10.3847/0004-637X/829/1/57](https://doi.org/10.3847/0004-637X/829/1/57)
- Bansal, A., Ichiki, K., Tashiro, H., & Matsuoka, Y. 2022, *Evolution of the mass relation between supermassive black holes and dark matter halos across the cosmic time*, arXiv, doi: [10.48550/arXiv.2206.01443](https://doi.org/10.48550/arXiv.2206.01443)
- Barai, P., & Pino, E. M. d. G. D. 2018, *Proceedings of the International Astronomical Union*, 14, 154, doi: [10.1017/S1743921318005525](https://doi.org/10.1017/S1743921318005525)
- Barth, A. J., Boizelle, B. D., Darling, J., et al. 2016, *ApJL*, 822, L28, doi: [10.3847/2041-8205/822/2/L28](https://doi.org/10.3847/2041-8205/822/2/L28)
- Barth, A. J., Ho, L. C., Filippenko, A. V., Rix, H.-W., & Sargent, W. L. W. 2001, *ApJ*, 546, 205, doi: [10.1086/318268](https://doi.org/10.1086/318268)
- Barth, A. J., Strigari, L. E., Bentz, M. C., Greene, J. E., & Ho, L. C. 2009, *ApJ*, 690, 1031, doi: [10.1088/0004-637X/690/1/1031](https://doi.org/10.1088/0004-637X/690/1/1031)
- Barth, A. J., Pancoast, A., Thorman, S. J., et al. 2011a, *ApJL*, 743, L4, doi: [10.1088/2041-8205/743/1/L4](https://doi.org/10.1088/2041-8205/743/1/L4)
- Barth, A. J., Nguyen, M. L., Malkan, M. A., et al. 2011b, *ApJ*, 732, 121, doi: [10.1088/0004-637X/732/2/121](https://doi.org/10.1088/0004-637X/732/2/121)
- Barth, A. J., Pancoast, A., Bennert, V. N., et al. 2013, *ApJ*, 769, 128, doi: [10.1088/0004-637X/769/2/128](https://doi.org/10.1088/0004-637X/769/2/128)
- Begelman, M. C., Volonteri, M., & Rees, M. J. 2006, *Monthly Notices of the Royal Astronomical Society*, 370, 289, doi: [10.1111/j.1365-2966.2006.10467.x](https://doi.org/10.1111/j.1365-2966.2006.10467.x)
- Beifiori, A., Courteau, S., Corsini, E. M., & Zhu, Y. 2012, *MNRAS*, 419, 2497, doi: [10.1111/j.1365-2966.2011.19903.x](https://doi.org/10.1111/j.1365-2966.2011.19903.x)
- Beifiori, A., Sarzi, M., Corsini, E. M., et al. 2009, *ApJ*, 692, 856, doi: [10.1088/0004-637X/692/1/856](https://doi.org/10.1088/0004-637X/692/1/856)
- Bekki, K., & Chiba, M. 2005, *Monthly Notices of the Royal Astronomical Society*, 356, 680, doi: [10.1111/j.1365-2966.2004.08510.x](https://doi.org/10.1111/j.1365-2966.2004.08510.x)
- Bender, R., Kormendy, J., Bower, G., et al. 2005, *ApJ*, 631, 280, doi: [10.1086/432434](https://doi.org/10.1086/432434)
- Bennert, V. N., Auger, M. W., Treu, T., Woo, J.-H., & Malkan, M. A. 2011, *ApJ*, 726, 59, doi: [10.1088/0004-637X/726/2/59](https://doi.org/10.1088/0004-637X/726/2/59)
- Bentz, M. C., & Katz, S. 2015, *PASP*, 127, 67, doi: [10.1086/679601](https://doi.org/10.1086/679601)
- Bentz, M. C., Denney, K. D., Cackett, E. M., et al. 2006, *ApJ*, 651, 775, doi: [10.1086/507417](https://doi.org/10.1086/507417)
- Bentz, M. C., Walsh, J. L., Barth, A. J., et al. 2010, *ApJ*, 716, 993, doi: [10.1088/0004-637X/716/2/993](https://doi.org/10.1088/0004-637X/716/2/993)
- Bentz, M. C., Horenstein, D., Bazhaw, C., et al. 2014, *ApJ*, 796, 8, doi: [10.1088/0004-637X/796/1/8](https://doi.org/10.1088/0004-637X/796/1/8)
- Berek, S. C., Eadie, G. M., Speagle, J. S., & Harris, W. E. 2023, *The Astrophysical Journal*, 955, 22, doi: [10.3847/1538-4357/ace7b7](https://doi.org/10.3847/1538-4357/ace7b7)
- Betancourt, M. 2018, *A Conceptual Introduction to Hamiltonian Monte Carlo*, arXiv. <http://arxiv.org/abs/1701.02434>
- Billingsley, P. 1995, *Probability and Measure* (Wiley)
- Blais-Ouellette, S., Amram, P., Carignan, C., & Swaters, R. 2004, *A&A*, 420, 147, doi: [10.1051/0004-6361:20034263](https://doi.org/10.1051/0004-6361:20034263)
- Boeker, T., van der Marel, R. P., & Vacca, W. D. 1999, *The Astronomical Journal*, 118, 831, doi: [10.1086/300985](https://doi.org/10.1086/300985)
- Bontà, E. D., Ferrarese, L., Miralda-Escudé, J., et al. 2006, *Proceedings of the International Astronomical Union*, 2, 355, doi: [10.1017/S174392130700542X](https://doi.org/10.1017/S174392130700542X)
- Bower, G. A., Green, R. F., Bender, R., et al. 2001, *ApJ*, 550, 75, doi: [10.1086/319730](https://doi.org/10.1086/319730)
- Boyce, H., Lützgendorf, N., Marel, R. P. v. d., et al. 2017, *The Astrophysical Journal*, 846, 14, doi: [10.3847/1538-4357/aa830c](https://doi.org/10.3847/1538-4357/aa830c)
- Boylan-Kolchin, M., Ma, C.-P., & Quataert, E. 2006, *Monthly Notices of the Royal Astronomical Society*, 369, 1081, doi: [10.1111/j.1365-2966.2006.10379.x](https://doi.org/10.1111/j.1365-2966.2006.10379.x)
- Braatz, J., Greenhill, L., Moran, J., Wilson, A., & Herrnstein, J. 1997, in *Bulletin of the American Astronomical Society*, Vol. 29, American Astronomical Society Meeting Abstracts, 1374
- Brinchmann, J., Charlot, S., White, S. D. M., et al. 2004, *Monthly Notices of the Royal Astronomical Society*, 351, 1151, doi: [10.1111/j.1365-2966.2004.07881.x](https://doi.org/10.1111/j.1365-2966.2004.07881.x)
- Bürkner, P.-C. 2017, *Journal of Statistical Software*, 80, 1, doi: [10.18637/jss.v080.i01](https://doi.org/10.18637/jss.v080.i01)
- Capetti, A., Marconi, A., Macchetto, D., & Axon, D. 2005, *A&A*, 431, 465, doi: [10.1051/0004-6361:20041701](https://doi.org/10.1051/0004-6361:20041701)

- Cappellari, M., Verolme, E. K., van der Marel, R. P., et al. 2002, *ApJ*, 578, 787, doi: [10.1086/342653](https://doi.org/10.1086/342653)
- Cappellari, M., Bacon, R., Davies, R. L., et al. 2008, in *IAU Symposium*, Vol. 245, *Formation and Evolution of Galaxy Bulges*, ed. M. Bureau, E. Athanassoula, & B. Barbuy, 215–218, doi: [10.1017/S1743921308017687](https://doi.org/10.1017/S1743921308017687)
- Cappellari, M., di Serego Alighieri, S., Cimatti, A., et al. 2009, *ApJL*, 704, L34, doi: [10.1088/0004-637X/704/1/L34](https://doi.org/10.1088/0004-637X/704/1/L34)
- Carpenter, B., Gelman, A., Hoffman, M. D., et al. 2017, *Journal of statistical software*, 76
- Cocato, L., Sarzi, M., Pizzella, A., et al. 2006, *MNRAS*, 366, 1050, doi: [10.1111/j.1365-2966.2005.09901.x](https://doi.org/10.1111/j.1365-2966.2005.09901.x)
- Collaboration, E. H. T., Akiyama, K., Alberdi, A., et al. 2022a, *The Astrophysical Journal Letters*, 930, L12, doi: [10.3847/2041-8213/ac6674](https://doi.org/10.3847/2041-8213/ac6674)
- . 2022b, *The Astrophysical Journal Letters*, 930, L13, doi: [10.3847/2041-8213/ac6675](https://doi.org/10.3847/2041-8213/ac6675)
- . 2022c, *The Astrophysical Journal Letters*, 930, L14, doi: [10.3847/2041-8213/ac6429](https://doi.org/10.3847/2041-8213/ac6429)
- . 2022d, *The Astrophysical Journal Letters*, 930, L15, doi: [10.3847/2041-8213/ac6736](https://doi.org/10.3847/2041-8213/ac6736)
- . 2022e, *The Astrophysical Journal Letters*, 930, L16, doi: [10.3847/2041-8213/ac6672](https://doi.org/10.3847/2041-8213/ac6672)
- . 2022f, *The Astrophysical Journal Letters*, 930, L17, doi: [10.3847/2041-8213/ac6756](https://doi.org/10.3847/2041-8213/ac6756)
- Collaboration, T. E. H. T., Akiyama, K., Alberdi, A., et al. 2019a, *The Astrophysical Journal Letters*, 875, L1, doi: [10.3847/2041-8213/ab0ec7](https://doi.org/10.3847/2041-8213/ab0ec7)
- . 2019b, *The Astrophysical Journal Letters*, 875, L2, doi: [10.3847/2041-8213/ab0c96](https://doi.org/10.3847/2041-8213/ab0c96)
- . 2019c, *The Astrophysical Journal Letters*, 875, L3, doi: [10.3847/2041-8213/ab0c57](https://doi.org/10.3847/2041-8213/ab0c57)
- . 2019d, *The Astrophysical Journal Letters*, 875, L4, doi: [10.3847/2041-8213/ab0e85](https://doi.org/10.3847/2041-8213/ab0e85)
- . 2019e, *The Astrophysical Journal Letters*, 875, L5, doi: [10.3847/2041-8213/ab0f43](https://doi.org/10.3847/2041-8213/ab0f43)
- . 2019f, *The Astrophysical Journal Letters*, 875, L6, doi: [10.3847/2041-8213/ab1141](https://doi.org/10.3847/2041-8213/ab1141)
- Collaboration, T. E. H. T., Akiyama, K., Algaba, J. C., et al. 2021a, *The Astrophysical Journal Letters*, 910, L12, doi: [10.3847/2041-8213/abe71d](https://doi.org/10.3847/2041-8213/abe71d)
- . 2021b, *The Astrophysical Journal Letters*, 910, L13, doi: [10.3847/2041-8213/abe4de](https://doi.org/10.3847/2041-8213/abe4de)
- Collins, C. A., Stott, J. P., Hilton, M., et al. 2009, *Nature*, 458, 603, doi: [10.1038/nature07865](https://doi.org/10.1038/nature07865)
- Cretton, N., & van den Bosch, F. C. 1999, *ApJ*, 514, 704, doi: [10.1086/306971](https://doi.org/10.1086/306971)
- Dalla Bontà, E., Ferrarese, L., Corsini, E. M., et al. 2009, *ApJ*, 690, 537, doi: [10.1088/0004-637X/690/1/537](https://doi.org/10.1088/0004-637X/690/1/537)
- Dashyan, G., & Dubois, Y. 2020, *Astronomy & Astrophysics*, 638, A123, doi: [10.1051/0004-6361/201936339](https://doi.org/10.1051/0004-6361/201936339)
- Davies, R. I., Thomas, J., Genzel, R., et al. 2006, *ApJ*, 646, 754, doi: [10.1086/504963](https://doi.org/10.1086/504963)
- Davis, T. A., Bureau, M., Cappellari, M., Sarzi, M., & Blitz, L. 2013, *Nature*, 494, 328, doi: [10.1038/nature11819](https://doi.org/10.1038/nature11819)
- de Francesco, G., Capetti, A., & Marconi, A. 2008, *A&A*, 479, 355, doi: [10.1051/0004-6361:20078570](https://doi.org/10.1051/0004-6361:20078570)
- De Lorenzi, F., Hartmann, M., Debattista, V. P., Seth, A. C., & Gerhard, O. 2013, *MNRAS*, 429, 2974, doi: [10.1093/mnras/sts545](https://doi.org/10.1093/mnras/sts545)
- de Souza, R. S., Hilbe, J. M., Buelens, B., et al. 2015a, *Monthly Notices of the Royal Astronomical Society*, 453, 1928, doi: [10.1093/mnras/stv1825](https://doi.org/10.1093/mnras/stv1825)
- de Souza, R. S., Cameron, E., Killedar, M., et al. 2015b, *Astronomy and Computing*, 12, 21, doi: [10.1016/j.ascom.2015.04.002](https://doi.org/10.1016/j.ascom.2015.04.002)
- den Brok, M., van de Ven, G., van den Bosch, R., & Watkins, L. 2014, *MNRAS*, 438, 487, doi: [10.1093/mnras/stt2221](https://doi.org/10.1093/mnras/stt2221)
- den Brok, M., Seth, A. C., Barth, A. J., et al. 2015, *ApJ*, 809, 101, doi: [10.1088/0004-637X/809/1/101](https://doi.org/10.1088/0004-637X/809/1/101)
- Denney, K. D., Watson, L. C., Peterson, B. M., et al. 2009, *ApJ*, 702, 1353, doi: [10.1088/0004-637X/702/2/1353](https://doi.org/10.1088/0004-637X/702/2/1353)
- Denney, K. D., Peterson, B. M., Pogge, R. W., et al. 2010, *ApJ*, 721, 715, doi: [10.1088/0004-637X/721/1/715](https://doi.org/10.1088/0004-637X/721/1/715)
- Devereux, N., Ford, H., Tsvetanov, Z., & Jacoby, G. 2003, *AJ*, 125, 1226, doi: [10.1086/367595](https://doi.org/10.1086/367595)
- Dietrich, M., Peterson, B. M., Grier, C. J., et al. 2012, *ApJ*, 757, 53, doi: [10.1088/0004-637X/757/1/53](https://doi.org/10.1088/0004-637X/757/1/53)
- Di Teodoro, E. M., McClure-Griffiths, N. M., Jameson, K. E., et al. 2019, *Monthly Notices of the Royal Astronomical Society*, 483, 392, doi: [10.1093/mnras/sty3095](https://doi.org/10.1093/mnras/sty3095)
- Do, T., Wright, S. A., Barth, A. J., et al. 2014, *The Astronomical Journal*, 147, 93, doi: [10.1088/0004-6256/147/4/93](https://doi.org/10.1088/0004-6256/147/4/93)
- Doroshenko, V. T., Sergeev, S. G., Klimanov, S. A., Pronik, V. I., & Efimov, Y. S. 2012, *MNRAS*, 426, 416, doi: [10.1111/j.1365-2966.2012.20843.x](https://doi.org/10.1111/j.1365-2966.2012.20843.x)
- Doroshenko, V. T., Sergeev, S. G., & Pronik, V. I. 2008, *Astronomy Reports*, 52, 442, doi: [10.1134/S1063772908060024](https://doi.org/10.1134/S1063772908060024)
- Du, P., Hu, C., Lu, K.-X., et al. 2014, *ApJ*, 782, 45, doi: [10.1088/0004-637X/782/1/45](https://doi.org/10.1088/0004-637X/782/1/45)
- Dullo, B. T., de Paz, A. G., & Knapen, J. H. 2021, *The Astrophysical Journal*, 908, 134, doi: [10.3847/1538-4357/abceae](https://doi.org/10.3847/1538-4357/abceae)

- Eadie, G. M., Harris, W. E., & Springford, A. 2022, *The Astrophysical Journal*, 926, 162, doi: [10.3847/1538-4357/ac33b0](https://doi.org/10.3847/1538-4357/ac33b0)
- Efstathiou, G. 2000, *Monthly Notices of the Royal Astronomical Society*, 317, 697, doi: [10.1046/j.1365-8711.2000.03665.x](https://doi.org/10.1046/j.1365-8711.2000.03665.x)
- Elliott, J., de Souza, R. S., Krone-Martins, A., et al. 2015, *Astronomy and Computing*, 10, 61, doi: [10.1016/j.ascom.2015.01.002](https://doi.org/10.1016/j.ascom.2015.01.002)
- Emsellem, E., Dejonghe, H., & Bacon, R. 1999, *MNRAS*, 303, 495, doi: [10.1046/j.1365-8711.1999.02210.x](https://doi.org/10.1046/j.1365-8711.1999.02210.x)
- Evans, N. H., & Peacock, B. 2000, *Measurement Science and Technology*, 12, 117, doi: [10.1088/0957-0233/12/1/702](https://doi.org/10.1088/0957-0233/12/1/702)
- Faber, S. M., Wegner, G., Burstein, D., et al. 1989, *The Astrophysical Journal Supplement Series*, 69, 763, doi: [10.1086/191327](https://doi.org/10.1086/191327)
- Faber, S. M., Tremaine, S., Ajhar, E. A., et al. 1997, *The Astronomical Journal*, 114, 1771, doi: [10.1086/118606](https://doi.org/10.1086/118606)
- Falcón-Barroso, J., Lyubenova, M., Ven, G. v. d., et al. 2017, *Astronomy & Astrophysics*, 597, A48, doi: [10.1051/0004-6361/201628625](https://doi.org/10.1051/0004-6361/201628625)
- Feller, W. 1968, *An Introduction to Probability Theory and Its Applications*, Vol. 1 (Wiley). <http://www.amazon.ca/exec/obidos/redirect?tag=citeulike04-20&path=ASIN/0471257087>
- Ferrarese, L., & Ford, H. C. 1999, *ApJ*, 515, 583, doi: [10.1086/307046](https://doi.org/10.1086/307046)
- Ferrarese, L., Ford, H. C., & Jaffe, W. 1996, *ApJ*, 470, 444, doi: [10.1086/177876](https://doi.org/10.1086/177876)
- Ferrarese, L., & Merritt, D. 2000, *The Astrophysical Journal*, 539, L9, doi: [10.1086/312838](https://doi.org/10.1086/312838)
- Ferré-Mateu, A., Mezcua, M., Trujillo, I., Balcells, M., & van den Bosch, R. C. E. 2015, *ApJ*, 808, 79, doi: [10.1088/0004-637X/808/1/79](https://doi.org/10.1088/0004-637X/808/1/79)
- Gao, F., Braatz, J. A., Reid, M. J., et al. 2016, *The Astrophysical Journal*, 834, 52, doi: [10.3847/1538-4357/834/1/52](https://doi.org/10.3847/1538-4357/834/1/52)
- Gao, F., Braatz, J. A., Reid, M. J., et al. 2016, *ApJ*, 817, 128, doi: [10.3847/0004-637X/817/2/128](https://doi.org/10.3847/0004-637X/817/2/128)
- Gebhardt, K., Rich, R. M., & Ho, L. C. 2005, *ApJ*, 634, 1093, doi: [10.1086/497023](https://doi.org/10.1086/497023)
- Gebhardt, K., Lauer, T. R., Kormendy, J., et al. 2001, *AJ*, 122, 2469, doi: [10.1086/323481](https://doi.org/10.1086/323481)
- Gebhardt, K., Lauer, T. R., Pinkney, J., et al. 2007, *ApJ*, 671, 1321, doi: [10.1086/522938](https://doi.org/10.1086/522938)
- Genzel, R., Eisenhauer, F., & Gillessen, S. 2010, *Reviews of Modern Physics*, 82, 3121, doi: [10.1103/RevModPhys.82.3121](https://doi.org/10.1103/RevModPhys.82.3121)
- Ghez, A. M., Salim, S., Weinberg, N. N., et al. 2008, *ApJ*, 689, 1044, doi: [10.1086/592738](https://doi.org/10.1086/592738)
- Gillessen, S., Eisenhauer, F., Trippe, S., et al. 2009, *ApJ*, 692, 1075, doi: [10.1088/0004-637X/692/2/1075](https://doi.org/10.1088/0004-637X/692/2/1075)
- Graham, A. W. 2007, *Monthly Notices of the Royal Astronomical Society*, 379, 711, doi: [10.1111/j.1365-2966.2007.11950.x](https://doi.org/10.1111/j.1365-2966.2007.11950.x)
- Graham, A. W., & Soria, R. 2018, *Monthly Notices of the Royal Astronomical Society*, doi: [10.1093/mnras/sty3398](https://doi.org/10.1093/mnras/sty3398)
- Greene, J. E. 2012, *Nature Communications*, 3, 1304, doi: [10.1038/ncomms2314](https://doi.org/10.1038/ncomms2314)
- Greene, J. E., & Ho, L. C. 2007, *The Astrophysical Journal*, 667, 131, doi: [10.1086/520497](https://doi.org/10.1086/520497)
- Greene, J. E., Strader, J., & Ho, L. C. 2020, *Annual Review of Astronomy and Astrophysics*, 58, 257, doi: [10.1146/annurev-astro-032620-021835](https://doi.org/10.1146/annurev-astro-032620-021835)
- Greene, J. E., van de Ven, G., van den Bosch, R., et al. 2011, *NOAO Proposal*, 77. <https://ui.adsabs.harvard.edu/abs/2011noao.prop...77G>
- Greene, J. E., Peng, C. Y., Kim, M., et al. 2010, *ApJ*, 721, 26, doi: [10.1088/0004-637X/721/1/26](https://doi.org/10.1088/0004-637X/721/1/26)
- Greene, J. E., Seth, A. C., Kim, M., et al. 2016, *ArXiv e-prints*. <https://arxiv.org/abs/1606.00018>
- Greenhill, L. J., Moran, J. M., & Herrnstein, J. R. 1997, *ApJL*, 481, L23, doi: [10.1086/310643](https://doi.org/10.1086/310643)
- Greenhill, L. J., Booth, R. S., Ellingsen, S. P., et al. 2003, *ApJ*, 590, 162, doi: [10.1086/374862](https://doi.org/10.1086/374862)
- Grier, C. J., Peterson, B. M., Pogge, R. W., et al. 2012, *ApJ*, 755, 60, doi: [10.1088/0004-637X/755/1/60](https://doi.org/10.1088/0004-637X/755/1/60)
- Grier, C. J., Martini, P., Watson, L. C., et al. 2013, *ApJ*, 773, 90, doi: [10.1088/0004-637X/773/2/90](https://doi.org/10.1088/0004-637X/773/2/90)
- Gültekin, K., Gebhardt, K., Kormendy, J., et al. 2014, *ApJ*, 781, 112, doi: [10.1088/0004-637X/781/2/112](https://doi.org/10.1088/0004-637X/781/2/112)
- Gültekin, K., Tremaine, S., Loeb, A., & Richstone, D. O. 2011, *ApJ*, 738, 17, doi: [10.1088/0004-637X/738/1/17](https://doi.org/10.1088/0004-637X/738/1/17)
- Gültekin, K., Richstone, D. O., Gebhardt, K., et al. 2009, *ApJ*, 698, 198, doi: [10.1088/0004-637X/698/1/198](https://doi.org/10.1088/0004-637X/698/1/198)
- Gültekin, K., King, A. L., Cackett, E. M., et al. 2019, *The Astrophysical Journal*, 871, 80, doi: [10.3847/1538-4357/aaf6b9](https://doi.org/10.3847/1538-4357/aaf6b9)
- Gültekin, K., Richstone, D. O., Gebhardt, K., et al. 2009, *The Astrophysical Journal*, 695, 1577, doi: [10.1088/0004-637X/695/2/1577](https://doi.org/10.1088/0004-637X/695/2/1577)
- Hagiwara, Y., Diamond, P. J., Nakai, N., & Kawabe, R. 2001, *The Astrophysical Journal*, 560, 119, doi: [10.1086/322416](https://doi.org/10.1086/322416)
- Haidar, H., Habouzit, M., Volonteri, M., et al. 2022, *The black hole population in low-mass galaxies in large-scale cosmological simulations*, Tech. Rep. arXiv:2201.09888, arXiv. <http://arxiv.org/abs/2201.09888>



- Hardin, J. W., Hardin, J. W., Hilbe, J. M., & Hilbe, J. 2007, *Generalized Linear Models and Extensions*, Second Edition (Stata Press)
- Häring, N., & Rix, H.-W. 2004, *ApJL*, 604, L89, doi: [10.1086/383567](https://doi.org/10.1086/383567)
- Harris, J., & Zaritsky, D. 2006, *The Astronomical Journal*, 131, 2514, doi: [10.1086/500974](https://doi.org/10.1086/500974)
- Heckman, T. M., & Best, P. N. 2014, *Annual Review of Astronomy and Astrophysics*, 52, 589, doi: [10.1146/annurev-astro-081913-035722](https://doi.org/10.1146/annurev-astro-081913-035722)
- Herrnstein, J. R., Moran, J. M., Greenhill, L. J., & Trotter, A. S. 2005, *ApJ*, 629, 719, doi: [10.1086/431421](https://doi.org/10.1086/431421)
- Hilbe, J. M., De Souza, R. S., & Ishida, E. E. 2017, *Bayesian models for astrophysical data: using R, JAGS, Python, and Stan* (Cambridge University Press)
- Hlavacek-Larrondo, J., Fabian, A. C., Edge, A. C., & Hogan, M. T. 2012, *Monthly Notices of the Royal Astronomical Society*, 424, 224, doi: [10.1111/j.1365-2966.2012.21187.x](https://doi.org/10.1111/j.1365-2966.2012.21187.x)
- Hoffman, M. D., & Gelman, A. 2011, *The No-U-Turn Sampler: Adaptively Setting Path Lengths in Hamiltonian Monte Carlo*, arXiv. <http://arxiv.org/abs/1111.4246>
- Houghton, R. C. W., Magorrian, J., Sarzi, M., et al. 2006, *MNRAS*, 367, 2, doi: [10.1111/j.1365-2966.2005.09713.x](https://doi.org/10.1111/j.1365-2966.2005.09713.x)
- Huré, J.-M., Hersant, F., Surville, C., Nakai, N., & Jacq, T. 2011, *A&A*, 530, A145, doi: [10.1051/0004-6361/201015062](https://doi.org/10.1051/0004-6361/201015062)
- Ishibashi, W., & Fabian, A. C. 2017, *Monthly Notices of the Royal Astronomical Society*, 472, 2768, doi: [10.1093/mnras/stx2212](https://doi.org/10.1093/mnras/stx2212)
- Jardel, J. R., Gebhardt, K., Shen, J., et al. 2011, *ApJ*, 739, 21, doi: [10.1088/0004-637X/739/1/21](https://doi.org/10.1088/0004-637X/739/1/21)
- Kamann, S., Wisotzki, L., Roth, M. M., et al. 2014, *A&A*, 566, A58, doi: [10.1051/0004-6361/201322183](https://doi.org/10.1051/0004-6361/201322183)
- Kamann, S., Husser, T.-O., Brinchmann, J., et al. 2016, *A&A*, 588, A149, doi: [10.1051/0004-6361/201527065](https://doi.org/10.1051/0004-6361/201527065)
- Kauffmann, G., Heckman, T. M., Tremonti, C., et al. 2003a, *Monthly Notices of the Royal Astronomical Society*, 346, 1055, doi: [10.1111/j.1365-2966.2003.07154.x](https://doi.org/10.1111/j.1365-2966.2003.07154.x)
- Kauffmann, G., Heckman, T. M., White, S. D. M., et al. 2003b, *Monthly Notices of the Royal Astronomical Society*, 341, 33, doi: [10.1046/j.1365-8711.2003.06291.x](https://doi.org/10.1046/j.1365-8711.2003.06291.x)
- Kelly, B. C. 2007, *ApJ*, 665, 1489, doi: [10.1086/519947](https://doi.org/10.1086/519947)
- Kollatschny, W., Ulbrich, K., Zetzl, M., Kaspi, S., & Haas, M. 2014, *A&A*, 566, A106, doi: [10.1051/0004-6361/201423901](https://doi.org/10.1051/0004-6361/201423901)
- Kondratko, P. T., Greenhill, L. J., & Moran, J. M. 2005, *ApJ*, 618, 618, doi: [10.1086/426101](https://doi.org/10.1086/426101)
- . 2008, *ApJ*, 678, 87, doi: [10.1086/586879](https://doi.org/10.1086/586879)
- Kormendy, J., Bender, R., & Cornell, M. E. 2011, *Nature*, 469, 374, doi: [10.1038/nature09694](https://doi.org/10.1038/nature09694)
- Kormendy, J., Drory, N., Bender, R., & Cornell, M. E. 2010, *ApJ*, 723, 54, doi: [10.1088/0004-637X/723/1/54](https://doi.org/10.1088/0004-637X/723/1/54)
- Kormendy, J., & Ho, L. C. 2013, *ARA&A*, 51, 511, doi: [10.1146/annurev-astro-082708-101811](https://doi.org/10.1146/annurev-astro-082708-101811)
- Kovačević, A., Popović, L. Č., Shapovalova, A. I., et al. 2014, *Advances in Space Research*, 54, 1414, doi: [10.1016/j.asr.2014.06.025](https://doi.org/10.1016/j.asr.2014.06.025)
- Krajnović, D., McDermid, R. M., Cappellari, M., & Davies, R. L. 2009, *MNRAS*, 399, 1839, doi: [10.1111/j.1365-2966.2009.15415.x](https://doi.org/10.1111/j.1365-2966.2009.15415.x)
- Krajnović, D., Cappellari, M., McDermid, R. M., et al. 2018, *Monthly Notices of the Royal Astronomical Society*, 477, 3030, doi: [10.1093/mnras/sty778](https://doi.org/10.1093/mnras/sty778)
- Kuo, C.-Y., Reid, M. J., Braatz, J. A., et al. 2018, *The Astrophysical Journal*, 859, 172, doi: [10.3847/1538-4357/aabff1](https://doi.org/10.3847/1538-4357/aabff1)
- Kuo, C. Y., Braatz, J. A., Condon, J. J., et al. 2011, *ApJ*, 727, 20, doi: [10.1088/0004-637X/727/1/20](https://doi.org/10.1088/0004-637X/727/1/20)
- Körding, E., Falcke, H., & Corbel, S. 2006, *Astronomy and Astrophysics*, 456, 439, doi: [10.1051/0004-6361:20054144](https://doi.org/10.1051/0004-6361:20054144)
- Laine, S., van der Marel, R. P., Lauer, T. R., et al. 2003, *The Astronomical Journal*, 125, 478, doi: [10.1086/345823](https://doi.org/10.1086/345823)
- Lauer, T. R., Faber, S. M., Richstone, D., et al. 2007, *ApJ*, 662, 808, doi: [10.1086/518223](https://doi.org/10.1086/518223)
- Lazzarini, M., Williams, B. F., Hornschemeier, A. E., et al. 2019, *The Astrophysical Journal*, 884, 2, doi: [10.3847/1538-4357/ab3f32](https://doi.org/10.3847/1538-4357/ab3f32)
- Leistedt, B., Mortlock, D. J., & Peiris, H. V. 2016, *Monthly Notices of the Royal Astronomical Society*, 460, 4258, doi: [10.1093/mnras/stw1304](https://doi.org/10.1093/mnras/stw1304)
- Lodato, G., & Bertin, G. 2003, *A&A*, 398, 517, doi: [10.1051/0004-6361:20021672](https://doi.org/10.1051/0004-6361:20021672)
- Lützgendorf, N., Kissler-Patig, M., Noyola, E., et al. 2011, *A&A*, 533, A36, doi: [10.1051/0004-6361/201116618](https://doi.org/10.1051/0004-6361/201116618)
- Lützgendorf, N., Kissler-Patig, M., Gebhardt, K., et al. 2013, *A&A*, 552, A49, doi: [10.1051/0004-6361/201220307](https://doi.org/10.1051/0004-6361/201220307)
- Lyubenova, M., van den Bosch, R. C. E., Côté, P., et al. 2013, *MNRAS*, 431, 3364, doi: [10.1093/mnras/stt414](https://doi.org/10.1093/mnras/stt414)
- Marconi, A., Axon, D. J., Capetti, A., et al. 2003, *ApJ*, 586, 868, doi: [10.1086/367764](https://doi.org/10.1086/367764)
- Martin-Navarro, I., & Mezcua, M. 2018, *Exploring the limits of AGN feedback: black holes and the star formation histories of low-mass galaxies*, doi: [10.3847/2041-8213/aab103](https://doi.org/10.3847/2041-8213/aab103)
- McConnell, N. J., & Ma, C.-P. 2013, *ApJ*, 764, 184, doi: [10.1088/0004-637X/764/2/184](https://doi.org/10.1088/0004-637X/764/2/184)
- McConnell, N. J., Ma, C.-P., Gebhardt, K., et al. 2011a, *Nature*, 480, 215, doi: [10.1038/nature10636](https://doi.org/10.1038/nature10636)

- McConnell, N. J., Ma, C.-P., Graham, J. R., et al. 2011b, *ApJ*, 728, 100, doi: [10.1088/0004-637X/728/2/100](https://doi.org/10.1088/0004-637X/728/2/100)
- McConnell, N. J., Ma, C.-P., Murphy, J. D., et al. 2012, *ApJ*, 756, 179, doi: [10.1088/0004-637X/756/2/179](https://doi.org/10.1088/0004-637X/756/2/179)
- McLaughlin, D. E., Anderson, J., Meylan, G., et al. 2006, *ApJS*, 166, 249, doi: [10.1086/505692](https://doi.org/10.1086/505692)
- McNamara, B. R., Kazemzadeh, F., Rafferty, D. A., et al. 2009, *The Astrophysical Journal*, 698, 594, doi: [10.1088/0004-637X/698/1/594](https://doi.org/10.1088/0004-637X/698/1/594)
- McNamara, B. R., & Nulsen, P. E. J. 2012, *New Journal of Physics*, 14, 055023, doi: [10.1088/1367-2630/14/5/055023](https://doi.org/10.1088/1367-2630/14/5/055023)
- Medling, A. M., Ammons, S. M., Max, C. E., et al. 2011, *ApJ*, 743, 32, doi: [10.1088/0004-637X/743/1/32](https://doi.org/10.1088/0004-637X/743/1/32)
- Merloni, A., Heinz, S., & Di Matteo, T. 2003, *Monthly Notices of the Royal Astronomical Society*, 345, 1057, doi: [10.1046/j.1365-2966.2003.07017.x](https://doi.org/10.1046/j.1365-2966.2003.07017.x)
- Merritt, D. 1999, *Black Holes and Galaxy Evolution*, Tech. Rep. arXiv:astro-ph/9910546, arXiv. <http://arxiv.org/abs/astro-ph/9910546>
- Merritt, D., Alexander, T., Mikkola, S., & Will, C. M. 2009, *Testing Properties of the Galactic Center Black Hole Using Stellar Orbits*, doi: [10.1103/PhysRevD.81.062002](https://doi.org/10.1103/PhysRevD.81.062002)
- Merritt, D., & Ferrarese, L. 2001, *The Astrophysical Journal*, 547, 140, doi: [10.1086/318372](https://doi.org/10.1086/318372)
- Merritt, D., Ferrarese, L., & Joseph, C. L. 2001, *Science*, 293, 1116, doi: [10.1126/science.1063896](https://doi.org/10.1126/science.1063896)
- Mezcua, M. 2017, *International Journal of Modern Physics D*, 26, 1730021, doi: [10.1142/S021827181730021X](https://doi.org/10.1142/S021827181730021X)
- Mezcua, M., Civano, F., Marchesi, S., et al. 2018a, *Monthly Notices of the Royal Astronomical Society*, 478, 2576, doi: [10.1093/mnras/sty1163](https://doi.org/10.1093/mnras/sty1163)
- Mezcua, M., Hlavacek-Larrondo, J., Lucey, J. R., et al. 2018b, *Monthly Notices of the Royal Astronomical Society*, 474, 1342, doi: [10.1093/mnras/stx2812](https://doi.org/10.1093/mnras/stx2812)
- Mezcua, M., & Sánchez, H. D. 2020, *The Astrophysical Journal*, 898, L30, doi: [10.3847/2041-8213/aba199](https://doi.org/10.3847/2041-8213/aba199)
- Miller, B. P., Gallo, E., Greene, J. E., et al. 2015, *The Astrophysical Journal*, 799, 98, doi: [10.1088/0004-637X/799/1/98](https://doi.org/10.1088/0004-637X/799/1/98)
- Nelder, J. A., & Wedderburn, R. W. M. 1972, *Journal of the Royal Statistical Society. Series A (General)*, 135, 370, doi: [10.2307/2344614](https://doi.org/10.2307/2344614)
- Neumayer, N., & Walcher, C. J. 2012, *Advances in Astronomy*, 2012, 15, doi: [10.1155/2012/709038](https://doi.org/10.1155/2012/709038)
- Nguyen, D. D. 2017, *Improved dynamical constraints on the mass of the central black hole in NGC 404*, Tech. Rep. arXiv:1712.02470, arXiv. <http://arxiv.org/abs/1712.02470>
- Nguyen, D. D., Seth, A. C., Reines, A. E., et al. 2014, *ApJ*, 794, 34, doi: [10.1088/0004-637X/794/1/34](https://doi.org/10.1088/0004-637X/794/1/34)
- Nowak, N., Saglia, R. P., Thomas, J., et al. 2008, *MNRAS*, 391, 1629, doi: [10.1111/j.1365-2966.2008.13960.x](https://doi.org/10.1111/j.1365-2966.2008.13960.x)
- . 2007, *MNRAS*, 379, 909, doi: [10.1111/j.1365-2966.2007.11949.x](https://doi.org/10.1111/j.1365-2966.2007.11949.x)
- Nowak, N., Thomas, J., Erwin, P., et al. 2010, *MNRAS*, 403, 646, doi: [10.1111/j.1365-2966.2009.16167.x](https://doi.org/10.1111/j.1365-2966.2009.16167.x)
- Oegerle, W. R., & Hoessel, J. G. 1991, *The Astrophysical Journal*, 375, 15, doi: [10.1086/170165](https://doi.org/10.1086/170165)
- Onishi, K., Iguchi, S., Davis, T. A., et al. 2016, *MNRAS*, submitted
- Onishi, K., Iguchi, S., Sheth, K., & Kohno, K. 2015, *ApJ*, 806, 39, doi: [10.1088/0004-637X/806/1/39](https://doi.org/10.1088/0004-637X/806/1/39)
- Onken, C. A., & Peterson, B. M. 2002, *ApJ*, 572, 746, doi: [10.1086/340351](https://doi.org/10.1086/340351)
- Onken, C. A., Valluri, M., Brown, J. S., et al. 2014, *ApJ*, 791, 37, doi: [10.1088/0004-637X/791/1/37](https://doi.org/10.1088/0004-637X/791/1/37)
- Pacucci, F., Loeb, A., Mezcua, M., & Martín-Navarro, I. 2018, *Glimmering in the dark: modeling the low-mass end of the  $M_{\bullet}$ - $\sigma$  relation and of the quasar luminosity function*, doi: [10.3847/2041-8213/aad8b2](https://doi.org/10.3847/2041-8213/aad8b2)
- Pastorini, G., Marconi, A., Capetti, A., et al. 2007, *A&A*, 469, 405, doi: [10.1051/0004-6361:20066784](https://doi.org/10.1051/0004-6361:20066784)
- Pei, L., Barth, A. J., Aldering, G. S., et al. 2014, *ApJ*, 795, 38, doi: [10.1088/0004-637X/795/1/38](https://doi.org/10.1088/0004-637X/795/1/38)
- Peterson, B. M., Ferrarese, L., Gilbert, K. M., et al. 2004, *ApJ*, 613, 682, doi: [10.1086/423269](https://doi.org/10.1086/423269)
- Peterson, B. M., Bentz, M. C., Desroches, L.-B., et al. 2005, *ApJ*, 632, 799, doi: [10.1086/444494](https://doi.org/10.1086/444494)
- Peterson, B. M., Grier, C. J., Horne, K., et al. 2014, *ApJ*, 795, 149, doi: [10.1088/0004-637X/795/2/149](https://doi.org/10.1088/0004-637X/795/2/149)
- Pignatelli, E., Salucci, P., & Danese, L. 2001, *MNRAS*, 320, 124, doi: [10.1046/j.1365-8711.2001.03942.x](https://doi.org/10.1046/j.1365-8711.2001.03942.x)
- Plotkin, R. M., Markoff, S., Kelly, B. C., Körding, E., & Anderson, S. F. 2012, *Monthly Notices of the Royal Astronomical Society*, 419, 267, doi: [10.1111/j.1365-2966.2011.19689.x](https://doi.org/10.1111/j.1365-2966.2011.19689.x)
- R Core Team. 2021, *R: A Language and Environment for Statistical Computing*, R Foundation for Statistical Computing, Vienna, Austria. <https://www.R-project.org/>
- Reines, A. E. 2022, *Nature Astronomy*, 6, 26, doi: [10.1038/s41550-021-01556-0](https://doi.org/10.1038/s41550-021-01556-0)
- Reines, A. E., & Volonteri, M. 2015, *ApJ*, 813, 82, doi: [10.1088/0004-637X/813/2/82](https://doi.org/10.1088/0004-637X/813/2/82)
- Rusli, S. P., Thomas, J., Saglia, R. P., et al. 2013, *AJ*, 146, 45, doi: [10.1088/0004-6256/146/3/45](https://doi.org/10.1088/0004-6256/146/3/45)
- Saglia, R. P., Opitsch, M., Erwin, P., et al. 2016, *ApJ*, 818, 47, doi: [10.3847/0004-637X/818/1/47](https://doi.org/10.3847/0004-637X/818/1/47)
- Salviander, S., & Shields, G. A. 2013, *The Astrophysical Journal*, 764, 80, doi: [10.1088/0004-637X/764/1/80](https://doi.org/10.1088/0004-637X/764/1/80)



- Sarzi, M., Rix, H.-W., Shields, J. C., et al. 2001, *ApJ*, 550, 65, doi: [10.1086/319724](https://doi.org/10.1086/319724)
- Scharwächter, J., McGregor, P. J., Dopita, M. A., & Beck, T. L. 2013, *MNRAS*, 429, 2315, doi: [10.1093/mnras/sts502](https://doi.org/10.1093/mnras/sts502)
- Schulze, A., & Gebhardt, K. 2011, *ApJ*, 729, 21, doi: [10.1088/0004-637X/729/1/21](https://doi.org/10.1088/0004-637X/729/1/21)
- Seth, A. C., Cappellari, M., Neumayer, N., et al. 2010, *ApJ*, 714, 713, doi: [10.1088/0004-637X/714/1/713](https://doi.org/10.1088/0004-637X/714/1/713)
- Seth, A. C., van den Bosch, R., Mieske, S., et al. 2014, *Nature*, 513, 398, doi: [10.1038/nature13762](https://doi.org/10.1038/nature13762)
- Shen, J., & Gebhardt, K. 2010, *ApJ*, 711, 484, doi: [10.1088/0004-637X/711/1/484](https://doi.org/10.1088/0004-637X/711/1/484)
- Shen, Y., Richards, G. T., Strauss, M. A., et al. 2011, *The Astrophysical Journal Supplement Series*, 194, 45, doi: [10.1088/0067-0049/194/2/45](https://doi.org/10.1088/0067-0049/194/2/45)
- Siopis, C., Gebhardt, K., Lauer, T. R., et al. 2009, *The Astrophysical Journal*, 693, 946, doi: [10.1088/0004-637X/693/1/946](https://doi.org/10.1088/0004-637X/693/1/946)
- Sisk-Reynés, J., Reynolds, C. S., Matthews, J. H., & Smith, R. N. 2022, *Monthly Notices of the Royal Astronomical Society*, 514, 2568, doi: [10.1093/mnras/stac1389](https://doi.org/10.1093/mnras/stac1389)
- Stalin, C. S., Jeyakumar, S., Coziol, R., Pawase, R. S., & Thakur, S. S. 2011, *MNRAS*, 416, 225, doi: [10.1111/j.1365-2966.2011.19030.x](https://doi.org/10.1111/j.1365-2966.2011.19030.x)
- Stinson, G. S., Dalcanton, J. J., Quinn, T., et al. 2009, *Monthly Notices of the Royal Astronomical Society*, 395, 1455, doi: [10.1111/j.1365-2966.2009.14555.x](https://doi.org/10.1111/j.1365-2966.2009.14555.x)
- Tadhunter, C., Marconi, A., Axon, D., et al. 2003, *MNRAS*, 342, 861, doi: [10.1046/j.1365-8711.2003.06588.x](https://doi.org/10.1046/j.1365-8711.2003.06588.x)
- Thater, S., Krajnovic, D., Cappellari, M., et al. 2019, *Astronomy & Astrophysics*, 625, A62, doi: [10.1051/0004-6361/201834808](https://doi.org/10.1051/0004-6361/201834808)
- Thomas, J., Ma, C.-P., McConnell, N. J., et al. 2016, *Nature*, 532, 340, doi: [10.1038/nature17197](https://doi.org/10.1038/nature17197)
- Tremaine, S., Gebhardt, K., Bender, R., et al. 2002, *ApJ*, 574, 740, doi: [10.1086/341002](https://doi.org/10.1086/341002)
- Tremonti, C. A., Heckman, T. M., Kauffmann, G., et al. 2004, *The Astrophysical Journal*, 613, 898, doi: [10.1086/423264](https://doi.org/10.1086/423264)
- Trotter, A. S., Greenhill, L. J., Moran, J. M., et al. 1998, *ApJ*, 495, 740, doi: [10.1086/305335](https://doi.org/10.1086/305335)
- Trump, J. R., Sun, M., Zeimann, G. R., et al. 2015, *The Astrophysical Journal*, 811, 26, doi: [10.1088/0004-637X/811/1/26](https://doi.org/10.1088/0004-637X/811/1/26)
- Valenti, E., Zoccali, M., Mucciarelli, A., et al. 2018, *Astronomy & Astrophysics*, 616, A83, doi: [10.1051/0004-6361/201832905](https://doi.org/10.1051/0004-6361/201832905)
- Valluri, M., Ferrarese, L., Merritt, D., & Joseph, C. L. 2005, *ApJ*, 628, 137, doi: [10.1086/430752](https://doi.org/10.1086/430752)
- van de Schoot, R., Depaoli, S., King, R., et al. 2021, *Nature Reviews Methods Primers*, 1, 1, doi: [10.1038/s43586-020-00001-2](https://doi.org/10.1038/s43586-020-00001-2)
- van den Bosch. 2016, *The Astrophysical Journal*, 831, 134, doi: [10.3847/0004-637X/831/2/134](https://doi.org/10.3847/0004-637X/831/2/134)
- van den Bosch, R., de Zeeuw, T., Gebhardt, K., Noyola, E., & van de Ven, G. 2006, *ApJ*, 641, 852, doi: [10.1086/500644](https://doi.org/10.1086/500644)
- van den Bosch, R. C. E., & de Zeeuw, P. T. 2010, *MNRAS*, 401, 1770, doi: [10.1111/j.1365-2966.2009.15832.x](https://doi.org/10.1111/j.1365-2966.2009.15832.x)
- van den Bosch, R. C. E., Gebhardt, K., Gültekin, K., Yıldırım, A., & Walsh, J. L. 2015, *ApJS*, 218, 10, doi: [10.1088/0067-0049/218/1/10](https://doi.org/10.1088/0067-0049/218/1/10)
- van den Bosch, R. C. E., Greene, J. E., Braatz, J. A., Constantin, A., & Kuo, C.-Y. 2016, *ApJ*, 819, 11, doi: [10.3847/0004-637X/819/1/11](https://doi.org/10.3847/0004-637X/819/1/11)
- van der Marel, R. P., & Anderson, J. 2010, *ApJ*, 710, 1063, doi: [10.1088/0004-637X/710/2/1063](https://doi.org/10.1088/0004-637X/710/2/1063)
- van der Marel, R. P., & van den Bosch, F. C. 1998, *AJ*, 116, 2220, doi: [10.1086/300593](https://doi.org/10.1086/300593)
- Van Wassenhove, S., Volonteri, M., Walker, M. G., & Gair, J. R. 2010, *Monthly Notices of the Royal Astronomical Society*, 408, 1139, doi: [10.1111/j.1365-2966.2010.17189.x](https://doi.org/10.1111/j.1365-2966.2010.17189.x)
- Volonteri, M., & Natarajan, P. 2009, *Monthly Notices of the Royal Astronomical Society*, 400, 1911, doi: [10.1111/j.1365-2966.2009.15577.x](https://doi.org/10.1111/j.1365-2966.2009.15577.x)
- Volonteri, M., Natarajan, P., & Gültekin, K. 2011, *The Astrophysical Journal*, 737, 50, doi: [10.1088/0004-637X/737/2/50](https://doi.org/10.1088/0004-637X/737/2/50)
- Walsh, J. L., Barth, A. J., Ho, L. C., & Sarzi, M. 2013, *ApJ*, 770, 86, doi: [10.1088/0004-637X/770/2/86](https://doi.org/10.1088/0004-637X/770/2/86)
- Walsh, J. L., Barth, A. J., & Sarzi, M. 2010, *ApJ*, 721, 762, doi: [10.1088/0004-637X/721/1/762](https://doi.org/10.1088/0004-637X/721/1/762)
- Walsh, J. L., van den Bosch, R. C. E., Barth, A. J., & Sarzi, M. 2012, *ApJ*, 753, 79, doi: [10.1088/0004-637X/753/1/79](https://doi.org/10.1088/0004-637X/753/1/79)
- Walsh, J. L., van den Bosch, R. C. E., Gebhardt, K., et al. 2015, *ApJ*, 808, 183, doi: [10.1088/0004-637X/808/2/183](https://doi.org/10.1088/0004-637X/808/2/183)
- . 2016, *ApJ*, 817, 2, doi: [10.3847/0004-637X/817/1/2](https://doi.org/10.3847/0004-637X/817/1/2)
- Wold, M., Lacy, M., Käuffl, H. U., & Siebenmorgen, R. 2006, *A&A*, 460, 449, doi: [10.1051/0004-6361:20053385](https://doi.org/10.1051/0004-6361:20053385)
- Xiao, T., Barth, A. J., Greene, J. E., et al. 2011, *The Astrophysical Journal*, 739, 28, doi: [10.1088/0004-637X/739/1/28](https://doi.org/10.1088/0004-637X/739/1/28)
- Yamauchi, A., Nakai, N., Sato, N., & Diamond, P. 2004, *PASJ*, 56, 605, doi: [10.1093/pasj/56.4.605](https://doi.org/10.1093/pasj/56.4.605)
- Yelda, S., Meyer, L., Ghez, A., & Do, T. 2013, *Astrometry in the Galactic center with the Thirty Meter Telescope*, doi: [10.12839/AO4ELT3.13371](https://doi.org/10.12839/AO4ELT3.13371)
- Yıldırım, A., van den Bosch, R. C. E., van de Ven, G., et al. 2015, *MNRAS*, 452, 1792, doi: [10.1093/mnras/stv1381](https://doi.org/10.1093/mnras/stv1381)

- Yoon, I. 2017, *Monthly Notices of the Royal Astronomical Society*, 466, 1987, doi: [10.1093/mnras/stw3171](https://doi.org/10.1093/mnras/stw3171)
- Zuur, A. F., Ieno, E. N., Walker, N. J., Saveliev, A. A., & Smith, G. M. 2009, in *Mixed effects models and extensions in ecology with R*, ed. A. F. Zuur, E. N. Ieno, N. Walker, A. A. Saveliev, & G. M. Smith, *Statistics for Biology and Health* (New York, NY: Springer), 261–293, doi: [10.1007/978-0-387-87458-6\\_11](https://doi.org/10.1007/978-0-387-87458-6_11)